The Role of Impurities during Creep and Superplasticity at Very Low Stresses

FARGHALLI A. MOHAMED

It is well documented that impurities play an important role in the deformation and fracture of polycrystalline materials. For example, the results of a number of studies have demonstrated that the presence of a very small of amount of impurities in polycrystalline materials can explain many phenomena such as temper embrittlement in steels, creep embrittlement, and enhancement of ductility in the intermetallic compound Ni_3Al. This article reviews the details of two high-temperature deformation phenomena whose characteristics are, according to very recent experimental evidence, influenced or controlled by impurities. The first phenomenon, micrograin superplasticity, deals with the ability of fine-grained materials ($d < 10$ μm, where d is the grain size) to exhibit extensive neck-free elongations during deformation at elevated temperatures above 0.5 T_m, where T_m is the melting point. The second phenomenon, Harper–Dorn creep, refers to the anomalous creep behavior of large-grained materials at very low stresses and temperatures near the melting point. It is shown that while these two phenomena are different in terms of the conditions of occurrence and the characteristics of deformation, they share three common features: (1) stresses applied to produce deformation are very small; (2) impurities control the deformation characteristics such as the shape of the creep curve, the value of the stress exponent, and the details of the substructure; and (3) boundaries play a key role during deformation.

I. INTRODUCTION

DESPITE their significance in providing basic information on deformation characteristics in terms of crystallography and despite their wide utilization in solid-state electronic devices, single crystals have limitations with respect to their strength, production, and size. Because of these limitations, most engineering materials are polycrystalline. The grain boundaries separating one crystal from another in a polycrystalline aggregate are structural discontinuities that represent regions of random misfit, ledges, and boundary dislocations.

As a result of their structures and high surface energy, grain boundaries influence the mechanical properties of materials. It is well documented that grain boundaries play an important role in the deformation and fracture of polycrystalline materials. At temperatures above about 0.5 T_m, where T_m is the melting point of the material, this role is reflected in several activities which include: (1) the occurrence of boundary sliding and migration,[1] (2) the formation of triple-point folds[2] and cavities,[3] and (3) the development of vacancy concentration gradients[4,5,6] as a result of tensile and compressive stresses on orthogonal boundaries (diffusional creep). In addition, the presence of boundaries serve as sites for the accumulation of impurities.[1] As a result of this process, referred to as boundary segregation, the impurity concentration at boundaries may be enhanced[1] relative to the matrix by a factor ranging from 10 to 10^3. Over the past three decades, it has been demonstrated that impurity segregation at boundaries can explain many phenomena such as temper embrittlement in steels,[3,7] creep embrittlement,[3,8] enhancement of ductility in the intermetallic compound Ni_3Al,[9] stress-corrosion cracking in commercial Al-Zr-Mg alloys,[10] and modification of grain-boundary diffusivity.[3]

This article reviews the recent progress made in rationalizing two high-temperature deformation phenomena that have received considerable attention over the past three decades and which, according to recent experimental evidence, involve some form of interaction between impurities and boundaries. The first phenomenon is associated with the high-temperature deformation of micrograined materials[11–14] that, upon tensile testing, exhibit extremely large elongations to fracture (micrograin superplastic deformation). The second phenomenon deals with the anomalous Newtonian creep behavior first reported in 1957 by Harper and Dorn in their study on the creep behavior of coarse-grained aluminum (Harper–Dorn creep).[15,16]

II. MICROGRAIN SUPERPLASTICITY

It has been demonstrated that micrograined materials ($d < 10$ μm, where d is the grain size) can exhibit extensive plastic deformation at elevated temperatures ($T > 0.5$ T_m, where T_m is the melting point), often without the formation of a neck prior to fracture. This high-temperature phenomenon is generally known as micrograin (structural) superplasticity. Micrograin superplastic behavior is indicated in tension tests by large elongations, usually greater than 300 pct and sometimes in excess of 2000 pct (Figure 1).

Micrograin superplasticity provides a low-cost method for manufacturing complex shapes, partly because large strains can be achieved without necking, and partly because the stresses required for deformation are generally small.

FARGHALLI A. MOHAMED, Professor, is with the Chemical Engineering and Materials Science Department, University of California, Irvine, CA 92697-2575.

This article is based on a presentation made in the workshop entitled "Mechanisms of Elevated Temperature Plasticity and Fracture," which was held June 27–29, 2001, in San Diego, CA, concurrent with the 2001 Joint Applied Mechanics and Materials Summer Conference. The workshop was sponsored by Basic Energy Sciences of the United States Department of Energy.

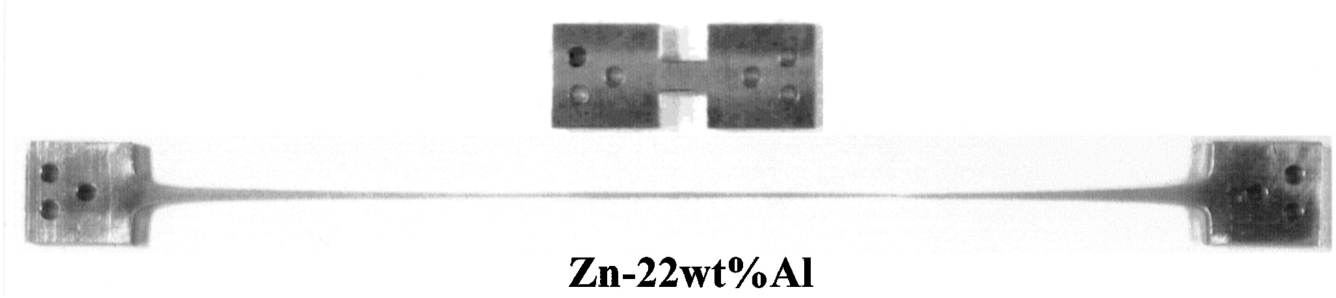

Fig. 1—Superplastic elongation in Zn-22 pct Al. The top specimen is untested. The other specimen (initial grain size, $d = 2.5$ μm) was pulled in tension at 473 K and initial strain of 10^{-2} s^{-1}.

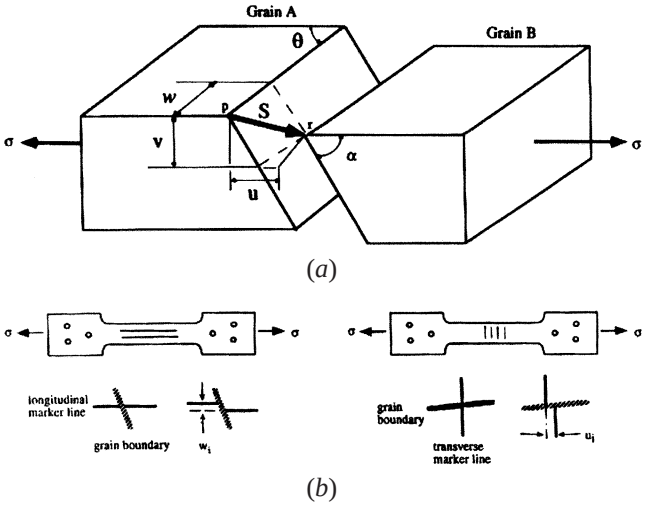

Fig. 2—(*a*) Schematic representation of GBS. (*b*) Schematic configuration of marker lines, longitudinal and transverse, and their offsets, *w* (perpendicular to stress axis) and *u* (parallel to the stress axis), respectively.

A. *Mechanical Behavior Associated with Micrograin Superplasticity*

Superplasticity is regarded as a creep phenomenon, since it has been observed at temperatures at or above 0.5 T_m. Accordingly, in studying the mechanical behavior of superplastic alloys, various investigations have focused on establishing the following four relationships, which define the basic deformation characteristics associated with a creep process: (1) the relationship between stress and strain rate,[17–25] (2) the relationship between strain rate or stress and temperature,[26,27,28] (3) the relationship between strain rate or stress and grain size, and (4) the relationship between strain contributed by boundary sliding and total strain.[29–40] In superplasticity experiments, the longitudinal offset (*u*) and/or the transverse offsets (*w*) have, in general, been considered in calculating the strain contribution from boundary sliding to total strain (Figures 2(a) and (b) provide details).

B. *Deformation Regions*

As a result of many studies on the aforementioned relationships, two findings are well documented. First, micrograin superplasticity is a diffusion-controlled process which can be represented by the following dimensionless equation:[41]

$$\frac{\dot{\gamma} kT}{DG\mathbf{b}} = A\left(\frac{\mathbf{b}}{d}\right)^s \left(\frac{\tau}{G}\right)^n \qquad [1a]$$

with

$$D = D_0 \exp\left(-\frac{Q}{RT}\right) \qquad [1b]$$

where $\dot{\gamma}$ is the shear creep rate, k is Boltzmann's constant, T is the absolute temperature, D is the diffusion coefficient that characterizes the dominant creep process, G is the shear modulus, $\mathbf{b}$ is the Burgers vector, A is a dimensionless constant, d is the grain size, s is the grain-size sensitivity, τ is the applied shear stress, n is the stress exponent, Q is the activation energy for the diffusion process that controls the creep behavior, and D_0 is the frequency factor for diffusion.

Second, the relationship between the stress (σ (tension) or τ (shear)) and steady-state creep rate ($\dot{\varepsilon}$ (tension) or $\dot{\gamma}$ (shear)) is often sigmoidal. In general, such a relationship is depicted by two types of presentation (Figure 3). In the first type of presentation, the data are plotted logarithmically as stress against strain. The slope of this plot yields the value of the strain-rate sensitivity (m). In the second type of presentation, the data are plotted logarithmically as strain rate against stress. The slope of such a plot represents the stress exponent (n). Under steady-state conditions, n is equal to $1/m$. Under creep conditions, the sigmoidal relationship is manifested by the presence of three regions:[42–48] region I (the low-stress region), region II (the intermediate-stress region), and region III (the high-stress region). As reported elsewhere,[42–48] the values of the stress exponent n ($n = (\partial \ln \dot{\gamma}/\partial \ln \tau)_{T,d}$) in regions I and III are higher than those in region II (where m is lower). In this review, the focus is placed on region I and its relation to region II. However, before reviewing recent data on region I, a summary of the characteristics of region III and region II is presented.

Region III (the high-stress region) is associated with the following characteristics: (1) the stress exponent n is higher than 3 (m is less than 0.33), (2) the apparent activation energy is higher than that for grain-boundary diffusion, (3) the dislocation activity in the interiors of grains is extensive, (4) changes in grain shape are appreciable, (5) the contribution of boundary sliding to total strain is about 20 pct, (6) the texture after deformation is appreciable, (7) the advent of region III is not sensitive to impurity level, and (8) the transition stresses from region II (the superplastic region) to region III closely correspond to those predicted from the equation that describes the dependence of the average

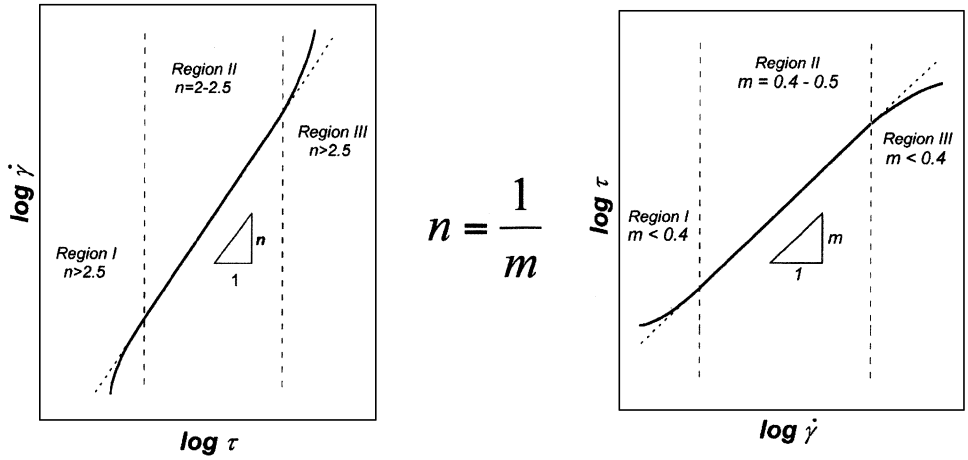

Fig. 3—Schematic presentation for the sigmoidal relationship between stress and strain rate (logarithmic scale), which often characterizes the formation behavior of micrograin superplastic alloys.

subgrain size (λ) formed during the creep of metals on applied stress.[41,49,51] This correspondence implies that region III occurs at higher stresses, where a stable subgrain structure begins to develop. It was suggested that the creep behavior of superplastic alloys in region III is controlled by the same type of dislocation process that is dominant in metals at high temperatures and whose creep rates are essentially insensitive to changes in grain size. However, this suggestion is not entirely satisfactory, since experimental results in a superplastic copper alloy[47] have revealed an inverse dependence of creep rate on grain size in region III. It seems most likely that region III is the result of the operation of some form of an intragrannular dislocation process, which is influenced by the presence of grain boundaries. One possibility is that as a result of boundary sliding, dislocations are emitted from triple points and boundary ledges, and that these dislocations interact with other lattice dislocations in the interiors of grains.

Region II (the intermediate-stress region) covers several orders of magnitude of strain rates and is characterized by a stress exponent of 1.5 to 2.5, an apparent activation energy (Q_a) that is close to that for boundary diffusion (Q_{gb}), and a grain-size sensitivity (s) of about 2. Also, in region II, maximum ductility occurs and the contribution of boundary sliding to the total strain is high[33–36] (50 to 70 pct), as shown schematically in Figure 4. Because of the former characteristic, region II is often referred to as the superplastic region.

Well-documented evidence has indicated that grain boundaries play an important role during superplastic deformation in region II. This evidence is based on several findings, including[11–14,52,53] (1) a fine and stable grain size of less than 10 μm represents a primary requirement for the observation of an extensive region II that covers several orders of magnitude of strain rates, (2) the lack of significant intragranular slip within the grain during deformation in region II, (3) strain rates measured during deformation are very sensitive to changes in grain size, and (4) the activation energy for superplastic flow is close to that anticipated for boundary diffusion. In addition to these findings, well-documented observations[11–14,53] on superplastic deformation have revealed that there is no appreciable change in grain shape and that grains remain equiaxed even at very large strains; that a change in the nature of boundary structure in a eutectoid composition steel from low-angle boundaries to high-angle ones lead to the observation of superplastic flow; and that the contribution of boundary sliding to the total strain is very significant at both small[33,37–40] and large elongations.[34]

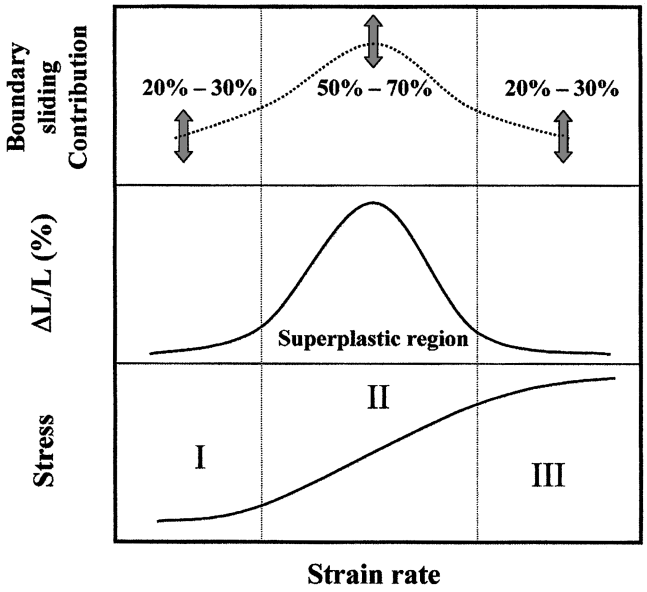

Fig. 4—Schematic correlations regarding the sigmoidal behavior, ductility, and contribution of boundary sliding to the total strain.

Combining the aforementioned findings and observations has led to the inference that boundary sliding represents an important feature of the deformation process that controls steady-state superplastic flow in region II. Such an inference was the basis of various deformation models,[54–60] in which the concept of boundary sliding accommodated either by diffusional flow or by dislocation motion[55–60] was adopted. Despite its attractive features (the occurrence of grain switching and rotation, the retention of the equiaxed grain structure, and the prediction of sigmoidal behavior), grain-boundary sliding (GBS) accommodated by diffusional flow,[54] as formulated by Ashby and Verrall, was in part criticized on the grounds that the diffusion paths characterizing the flow of material in the model are not physically

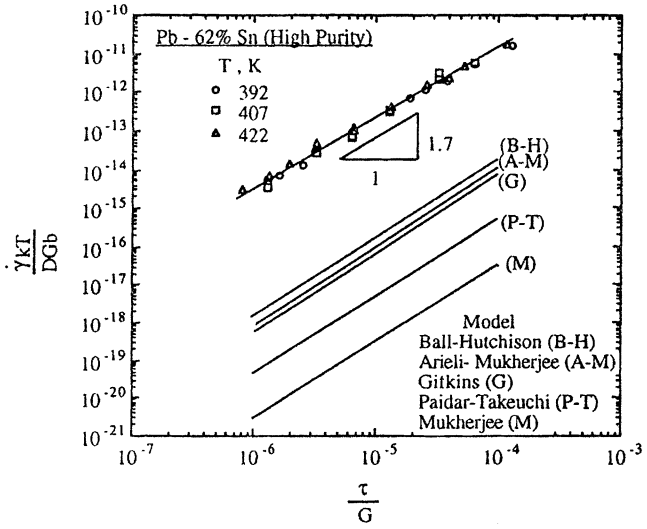

Fig. 5—Comparison between the predictions of various models describing GBS accommodated by dislocation motion and the experimental data for Pb-62 pct Sn. Data were taken from Ref. 62.

realistic. Details and assumptions in the models based on GBS accommodated by dislocation motion[55–60] are different (Table II). However, despite these differences, all of the models can be described by a rate-controlling equation that has the following form:

$$\dot{\gamma} = C \frac{D_0 G \mathbf{b}}{kT} \left(\frac{\mathbf{b}}{d}\right)^2 \left(\frac{\tau}{G}\right)^2 \exp\left(\frac{-Q_{gb}}{RT}\right) \qquad [2]$$

where C is a constant that can be estimated from the details of each model; the values of C are given elsewhere.[61,62] It has been reported[61,62] that the agreement between the values of the experimental creep rates in region II and those rates predicted from various models represented by Eq. [2] is not satisfactory. For example, Figure 5 shows the presence of a discrepancy of three to four orders of magnitude in the normalized creep rate between GBS models and the data on Pb–62 pct Sn. However, the fact that the concept of boundary sliding accommodated by some form of dislocation motion is successful in predicting the correct stress, temperature, and grain-size dependencies characterizing region II indicates the significance of boundary sliding as a key element in the process of describing the steady-state process controlling region II.

An important comment is in order regarding the contribution of boundary sliding to the total strain (ξ) in region II. The value of ξ in this region is in the range from 50 to 70 pct. This suggests that there is a missing strain of about 30 to 50 pct. This missing strain is too large to be explained in terms of diffusional creep and/or dislocation motion, in view of two well-documented observations related to superplastic deformation: the contribution of diffusional creep to the total strain is not significant,[63] and the strain produced by lattice dislocations is negligible.[64] Recently, Langdon[65] has argued that boundary sliding and the associated accommodation process account for essentially all strain produced during superplastic flow in region II, *i.e.*, there is no missing strain. His argument[65] is based on an analysis of the process of measuring sliding using marker lines parallel to the tensile axis in a two-dimensional array of hexagonal grains. Such an analysis[65] has led to the prediction that ξ exhibits a minimum value of 45 pct when sliding is not accommodated and assumes a maximum value of 90 pct under the condition that sliding is fully accommodated. On the basis of this prediction, Langdon[65] has concluded that since the accommodation of sliding is not fully required at the surface of a tensile specimen, the experimental values of ξ obtained from surface marker lines are expected to be close to the lower bound of the range of 45 to 90 pct.

C. *Region I (Low-Stress Region)*

In recent years, considerable attention has been focused on the creep behavior of superplastic alloys in region I. This attention has been motivated not only by the desire to identify the origin of region I but also by other important factors. First, an understanding of the origin of the low-stress region (region I) during superplastic flow is likely to shed light on the details of the deformation process that controls the intermediate-stress region (the superplastic region or region II). Second, information on superplastic flow at low stresses is important in defining microscopic characteristics and theoretical approaches that may be used to evaluate flow processes in the mantle of the Earth. Third, it is well recognized that the presence of cavities during superplasticity may impose a serious limitation on the mechanical properties of components prepared by superplastic forming. A solution of this problem necessitates a detailed understanding of the cavitation process in superplastic alloys over wide ranges of experimental conditions, including low stresses.

Early explanations for the origin of region I were centered around the following: (1) the operation of temperature-insensitive threshold-stress processes,[54,58,66,67] (2) the emergence of a new deformation mechanism,[42–44,57] or (3) the occurrence of concurrent grain growth.[68,69] However, as concluded elsewhere,[24] these explanations are not entirely consistent with available experimental evidence. Explanations (1) and (2) have been ruled out on the grounds that they cannot account for the higher activation energy measured in region I.[43,44,47,48] While explanation (3) is applicable in some cases, experimental evidence has shown the presence of a well-defined region I under experimental conditions involving negligible grain growth.[45,46]

Vaidy *et al.*[70] and Misro and Mukherjee[71] reported that region I did not exist in Zn-22 pct Al and that the creep characteristics of the alloy at very low stresses are consistent with those associated with boundary diffusional creep (Coble creep). This behavior was predicted[41] by Bird *et al.*: a transition from the superplastic region (region II) to Coble creep with decreasing applied stress. Although no other investigators have provided additional confirmation for the dominance of Coble creep in superplastic alloys at very low stresses, Prabir *et al.*[60] reported that the creep rates of Zn-22 pct Al doped with 400 ppm of Fe under the lowest stresses at 433 K exhibit values which were higher than those based on the extrapolation of the data in region I. Prabir *et al.* have suggested that such an experimental deviation from region I may be the result of an additive contribution from Coble creep to superplastic flow in Zn-22 pct Al.

D. *The Sensitivity of Region I Behavior to Impurities*

Recent experimental data have revealed[24,38–40,61,72–81] that the impurity level and type can significantly influence

region I behavior in superplastic alloys; neither steady-state deformation in region II (the superplastic region) nor the advent of region III appears to be sensitive to impurities (level or type). This evidence is manifested in part by the following observations regarding creep behavior and boundary sliding.

1. *Creep characteristics*

Data from several creep investigations on microgram superplasticity have shown that creep characteristics in region I are controlled not only by impurity level but also by its type. This finding has been demonstrated by the following experimental observations: (1) Zn-22 pct Al and Pb-62 pct Sn do not exhibit a region I when the level of impurities in both alloys is reduced to about 6 ppm[24,25,72] (compare Figure 6(a) with 6(b)); (2) for constant temperature, the transition between region II and region I is transposed to lower strain rates with a decreasing level of impurities; (3) the apparent stress exponent and the apparent activation energy for creep in region I, unlike those in region II, are sensitive to impurity content[24] for Zn-22 pct Al (Figure 6(c)); and (4) region I is absent in Zn-22 pct Al when the alloy is doped with Cu,[77] whereas this region is observed when the alloy is doped with a comparable atomic level of Fe[78] (Figure 6(d)).

2. *Boundary sliding*

Recent data on boundary sliding in Zn-22 pct Al have revealed[39] that the values of the contribution of boundary sliding to the total strain (ξ) at low strain rates (region I), unlike those at intermediate and high strain rates (region II and region III, respectively), are affected by the presence of impurities. This finding is reflected in several observations (Figure 7(a)) regarding the sliding behavior of three grades of Zn-22 pct Al that contained contain 180 ppm (grade 1), 100 ppm (grade 2), and 6 ppm (grade 3, a high-purity grade) of impurities. First, for all three grades, ξ exhibits the same value of 20 pct at high strain rates. Second, for grade 3 (high-purity Zn-22 pct Al), the ξ value at low strain rates is not only significant (61 pct), but also comparable to that at intermediate strain rates ($\sim$60 pct). Third, at the same strain rate in region I, the values of ξ in grades 1 and 2 are less than that in grade 3. Finally, at the same strain rate in region I, ξ in grade 1 (180 ppm of impurities) is less than that in grade 2 (100 ppm of impurities).

In addition, it has been reported[38] that the presence of Cd in Pb-62 pct Sn affects the values of the contribution of boundary sliding to the total strain at low strain rates (region I). This finding is manifested in the following observations (Figure 7(b)) regarding the sliding behavior of Pb-62 pct Sn doped with 890 ppm of Cd (grade 1) and high-purity Pb-62 pct Sn (grade 2): (1) for both grades, ξ exhibits essentially the same values at high strain rates and intermediate strain rates, (2) for grade 1, the value of ξ (31 pct) at low strain rates is less than that at intermediate strain rates (50 pct), and (3) for grade 2 (high-purity grade), ξ at low strain rates is not only significant (50 pct), but is also comparable to that at intermediate strain rates ($\sim$50 pct).

E. *Origin of Region I*

Experimental evidence appears to suggest that the deformation process controlling region I is not independent of that controlling region II. The interpretation of region I in terms of a new independent deformation process[42–44,57] seems to be consistent with some of the mechanical characteristics of this region. However, the origin and exact nature of such a low-stress process, in view of the high stress exponent ($n = 3$ to 5), the high activation energy ($Q > Q_{gb}$), the strong grain-size dependence ($s \sim 2$), and the absence of significant dislocation activity are not clear. In addition, investigators reported different values for the stress exponent ($n = 3$ to 5) and the activation energy ($Q > Q_{gb}$) for region I.

Combining the aforementioned suggestion with the finding that the deformation mechanism in region II involves boundary sliding and recent experimental evidence that impurities influence the creep of region I leads to the following possibility: region I behavior arises from some form of interaction between impurities and boundary sliding or its accommodation processes that include boundary migration, dislocation motion, diffusional flow, or cavitation (Figure 8). At present, based on an analysis of experimental data and an examination of theoretical considerations, two inferences can be made. First, models based on an impurity-controlled boundary migration[82] and dislocation viscous glide[24,83] do not provide entirely satisfactorily interoperations of the characteristics of region I in terms of an impurity effect (Figure 8). However, one cannot rule out the possibility that accommodation processes such as boundary migration and dislocation motion may be influenced by the presence of impurities and, as a result, they may play a role during superplastic deformation in region I. For example, the decrease in the contribution of boundary sliding to the total stain was explained[38,39,40] in terms of the effect of impurities on boundary migration and dislocation motion. Second, the operation of a threshold-stress process whose origin is related to impurity segregation at boundaries provides the most likely explanation for the sensitivity of region I behavior to the presence of an impurity.

F. *Impurity-dominated threshold stress for sliding*

It has been suggested[84,85] that the sensitivity of region I to the presence of impurities can be accounted for by a model that is based on boundary sliding and that incorporates a threshold stress. The model involves the following conditions: (1) the movement of appropriate boundary dislocations[12–14,54,65] produces boundary sliding, which plays the document role in the superplastic deformation processes, (2) impurity atoms are able to segregate to boundaries,[1,11,82] (3) such segregation occurs preferentially at boundary dislocations, resulting in dislocation pinning, and (4) under the conditions of strong binding between impurity atoms and dislocations and very low mobility of impurity atoms, a threshold stress must be exceeded before boundary dislocations can break away from the impurity atmosphere and produce sliding.

G. *Consistency between the Concept of Segregation and Experimental Trends*

The aforementioned proposed concept that region I behavior may be a consequence of the operation of a threshold-stress process whose origin is related to the segregation of impurity atoms at boundaries and their interaction with boundary dislocations appears to be in agreement with the present experimental evidence. This agreement between the

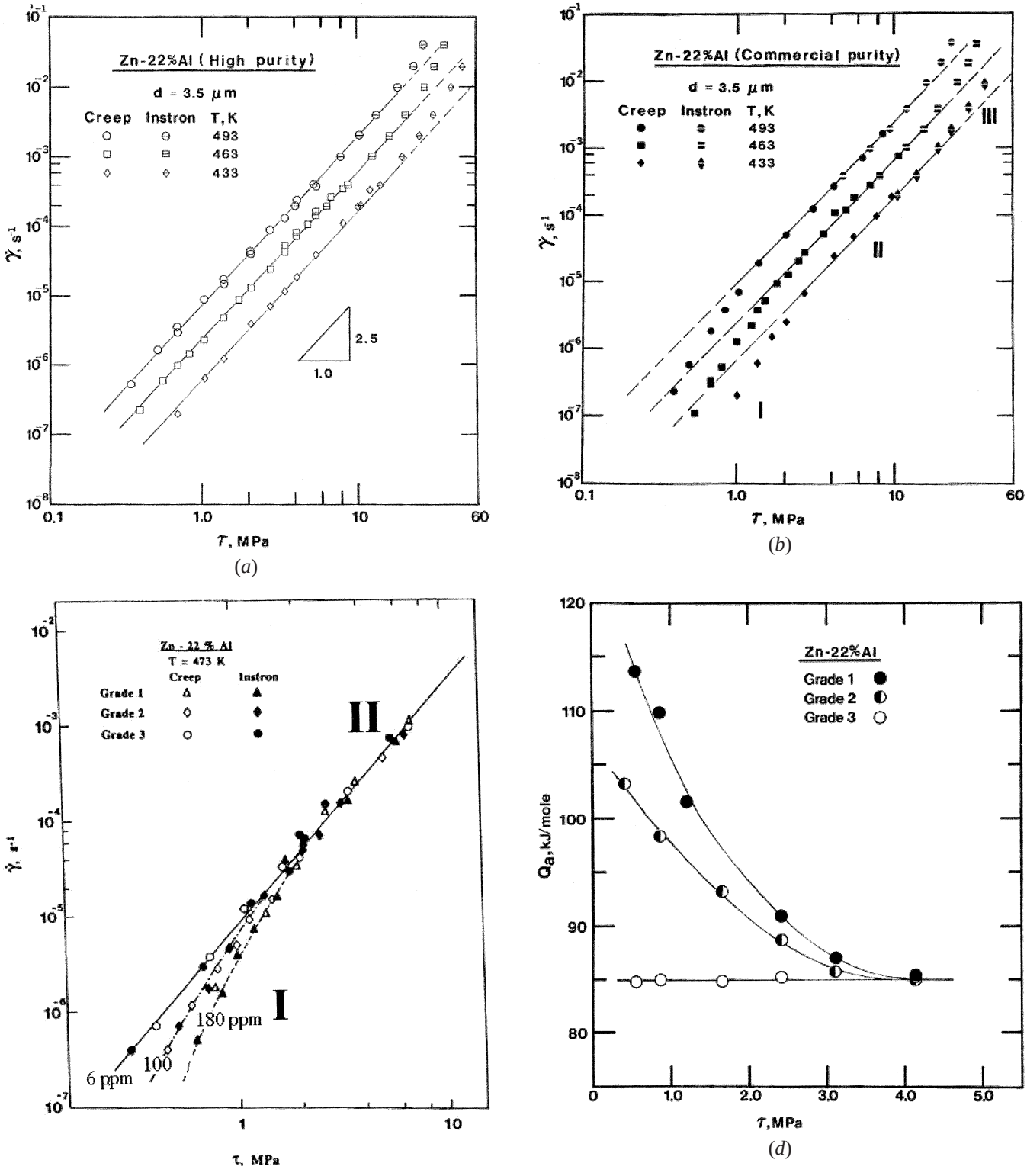

Fig. 6—(*a*) Shear strain rate *vs* shear stress (logarithmic scale) for high-purity Zn-22 pct Al (6 ppm of impurities) having a grain size of 3.5 mm at various temperatures. Region I (low-stress region) is absent. Data were taken from Ref. 72. (*b*) Shear strain rate *vs* shear stress (logarithmic scale) for commercial purity Zn-22 pct Al (180 ppm of impurities) having a grain size of 3.5 mm at various temperatures. Region I (low-stress region) is present. Data were taken from Ref. 72. (*c*) Shear strain rate *vs* shear stress (logarithmic scale) for three grades of Zn-22 pct Al (180 ppm of impurities) having a grain size of 2.5 mm at various temperatures: grades 1, 2, and 3 contain 180, 100, and 6 ppm of impurities, respectively. (*d*) The dependence of the average apparent activation energy on stress for grades 1, 2, and 3 of Zn-22 pct Al containing 180, 100, and 6 ppm of impurities, respectively (grain size = 2.5 μm). Data were taken from Ref. 61.

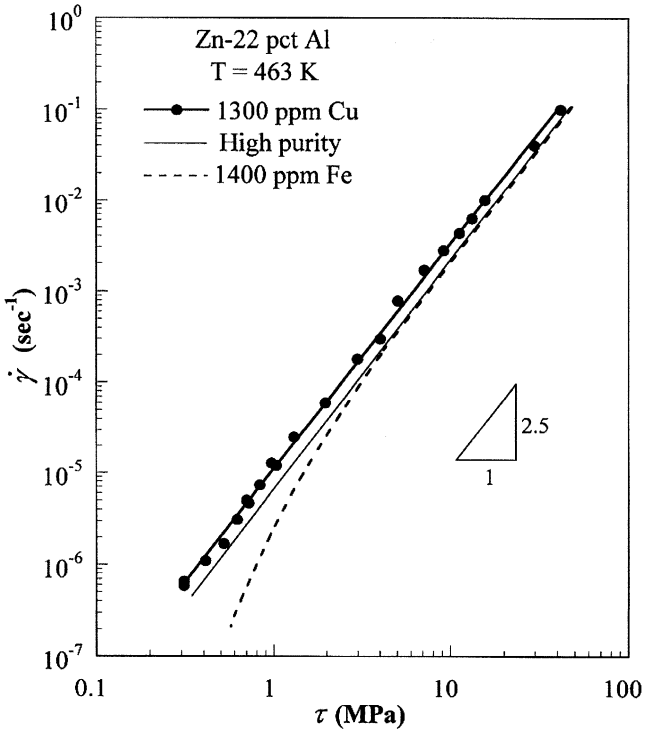

(*e*)

Fig. 6—Continued. (*e*) Shear strain rate *vs* shear stress (logarithmic scale) for high-purity Zn-22 pct Al, Zn-22 pct Al-0.1 pct Cu (grade Cu), and Zn-22 pct Al-0.14 pct Fe (grade Fe). Region I is absent in both high-purity Zn-22 pct Al and grade Cu, while it is present in grade Fe. Data were taken from Refs. 61, 77, and 78.

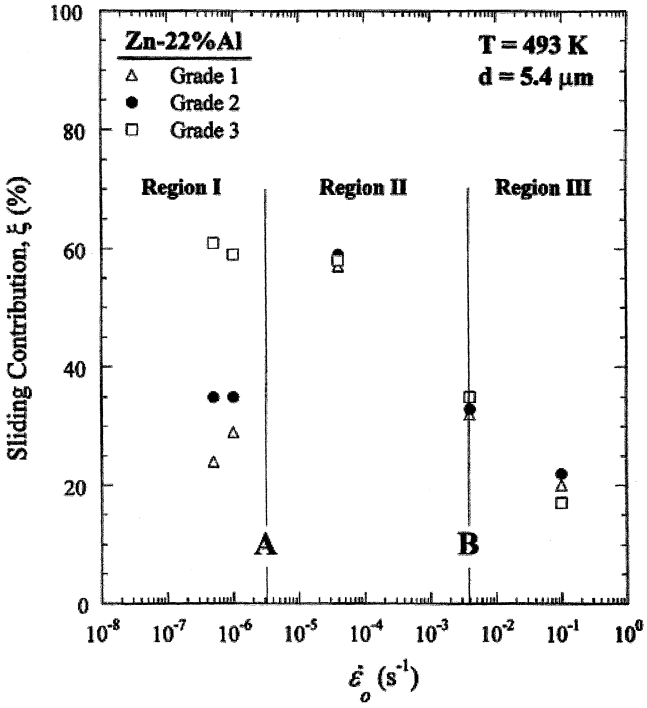

(*a*)

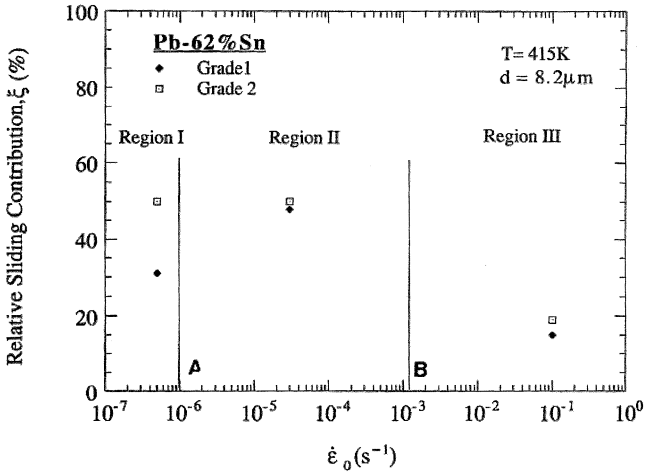

(*b*)

Fig. 7—(*a*) The contribution of boundary sliding to the total strain, ξ, as a function of strain rates for grades 1, 2, and 3 of Zn-22 pct Al containing 180, 100, and 6 ppm of impurities, respectively. Data were taken from Ref. 39. (*b*) The contribution of boundary sliding to the total strain, ξ, as a function of strain rate for grade Pb-62 pct Sn doped with 890 ppm Cd (grade 1) and high-purity Pb-62 pct Sn (grade 2). Data were taken from Ref. 38.

prediction of the concept and the trend of experimental data is described subsequently with regard to the following.

1. *Threshold stress*

Recent creep data reported for several grades of Zn-22 pct Al containing different levels of impurities,[24,61,72,77] in particular Fe, have revealed the presence of a threshold stress whose characteristics are consistent with various phenomena associated with boundary segregation. First, no threshold stress (τ_0) is observed for superplastic flow in high-purity Zn-22 pct Al[24,72] (Figure 9(a)). A similar trend for high-purity Pb-62 pct Sn was reported.[25] As demonstrated elsewhere,[24,62,61,72,77] τ_0 is determined from experimental creep data obtained for a superplastic alloy by plotting as $\dot{\gamma}^{1/n}$ ($n = 2.5$) against τ at a single temperature on a double linear scale and extrapolating the resultant line to a zero strain rate. Second, according to the experimental data reported for superplastic alloys,[24,62,61,72,77] the temperature dependence of the threshold stress is described by the following equation:

$$\frac{\tau_0}{G} = B_0 \exp\,(Q_0/RT) \qquad [3a]$$

where B_0 is a constant, and Q_0 is an activation-energy term. The plot of Figure 9(b) in which experimental data on the threshold-stress behavior of several grades of Zn-22 pct Al doped with Fe are plotted as τ_0/G *vs* $1/T$ on a logarithmic scale, provides a graphical presentation for the previous relation. Equation [3a] resembles in form the following equation,[1] which gives, to a first approximation, the concentration of impurity atoms segregated to boundaries (c) as a function of temperature:

$$c = c_0 \exp\,(W/RT) \qquad [3b]$$

where c_0 is the average concentration of an impurity, and W is the interaction energy between a boundary and a solute atom. Finally, the threshold stress appears to approach a limiting value for Fe concentrations above 120 ppm with increasing Fe levels (Figure 5(b)). It has been suggested[61]

$$\dot{\gamma} = A\left(\frac{b}{d}\right)^2 e^{-Q}\left(\frac{\tau}{G}\right)^n \quad \text{Region I: } n > 3\ Q > Q_{gb},\ s = 2$$

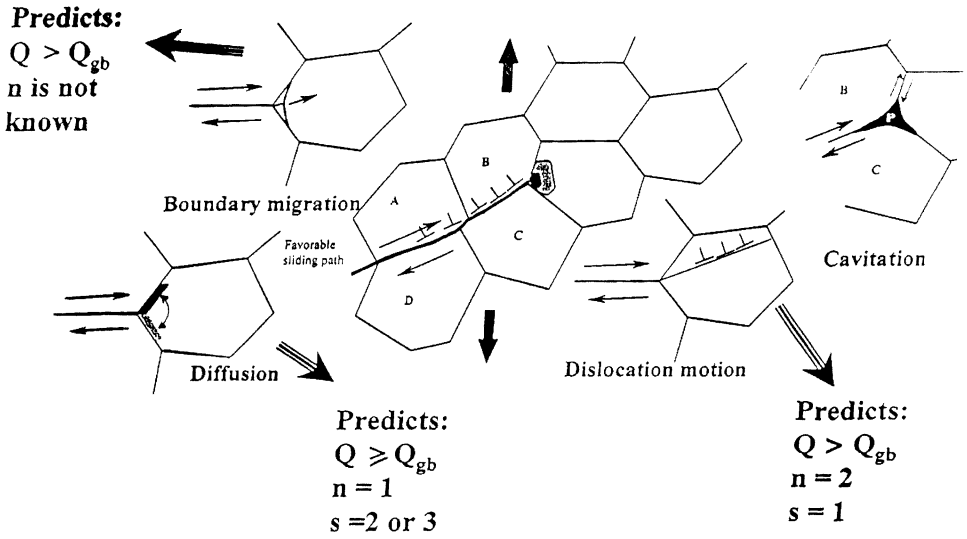

Fig. 8—Schematic presentation of boundary sliding and its accommodation processes. Included in the figure are the equation describing region I (the low-stress region of the sigmoidal behavior in micrograin superplastic alloys) and the rate equations characterizing these accommodation processes under the condition of impurity control.

that this Fe level (120 ppm) most likely represents the concentration at which boundary sites available for Fe segregation approach a saturation limit.

2. *Cavitation*

Experimental results have revealed the following observations:[73,74,75] (1) cavities are not observed in high-purity Zn-22 pct Al, and (2) the extent of cavitation in Zn-22 pct Al depends on the impurity content of the alloy. Figure 10 illustrates these observations. The observed correlation between the level of impurities and the extent of cavitation in Zn-22 pct Al is most probably related to effects associated with the presence of excessive impurities[3] at boundaries as a result of their segregation; the presence of excessive impurities at boundaries may lead to accelerated cavitation rates through processes that are discussed in detail elsewhere.[3]

It was reported that for approximately the same Fe concentration, the presence of other impurities in Zn-22 pct Al has the effect of increasing both the value of the threshold stress[61] and the extent of cavitation.[75] This characteristic is most likely a reflection of synergistic effects that are associated with impurity segregation at boundaries.[86,87,88]

A recent investigation[78] was conducted to study the effect of Cu, as a selected impurity, on superplastic deformation and cavitation in Zn-22 pct Al. The results have shown that cavitation is not extensive in Zn-22 pct Al doped with 1300 ppm of Cu (Figure 10). This characteristic is essentially similar to that reported[73] for high-purity Zn-22 pct Al, but is different from that documented for a grade of the alloy[75] containing a comparable atomic concentration of Fe (grade Fe, shown in Figure 10). This observation appears to be in line with the expectation that impurities vary greatly in their tendency to segregate at boundaries. In addition, the observation has suggested that Cu, unlike Fe, has little or no tendency to segregate at boundaries.

3. *Former alpha boundaries*

Former alpha boundaries (FαBs) are residual grain boundaries which develop in Zn-22 pct Al during a heat treatment which is normally applied to produce the fine structure necessary for micrograin superplasticity.[76,78–81] They represent domains consisting of fine elongated α grains, which encompass groups of fine α (Al-rich) and β (Zn-rich) phases (the superplastic microstructure). These characteristics are illustrated in Figure 11. It has recently been demonstrated that the kinetics of FαB domain growth, like that of normal grain growth, is controlled by impurities.[78–81] (Figure 11). This observation, which indicates that FαBs, like grain boundaries, serve as favorable sites for impurity segregation, has presented an approach to examine the tendency of different impurity atoms to segregate at boundaries as a function of their level and type. The significance of this approach may be appreciated when it is recognized that it is not feasible to directly examine impurity segregation at boundaries in superplastic alloys. In general, direct examination of boundary segregation requires the application of spectroscopic techniques, such as Auger spectroscopy, in which samples are fractured in vacuum and exposed grain boundaries are examined for segregation. In the case of materials that exhibit a ductile-to-brittle transition, *in-situ* fracture is produced by a combination of sample cooling and impact fracture. However, since superplastic alloys such as Zn-22 pct Al samples do not exhibit low-temperature brittleness, the procedure is not feasible to propagate intergranular failure.

Figure 12 shows that for five grades of Zn-22 pct Al, the

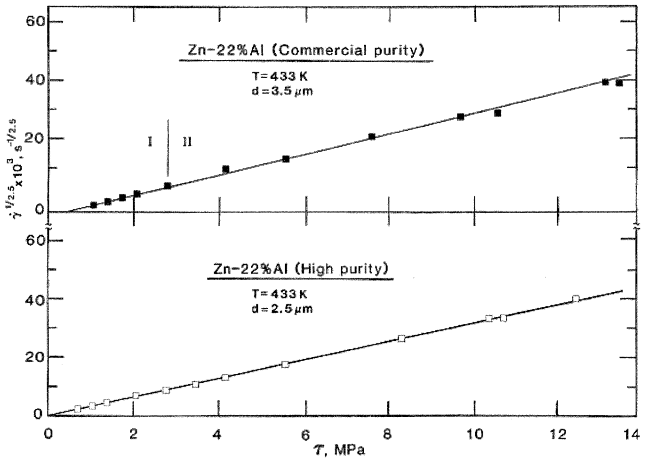

(*a*)

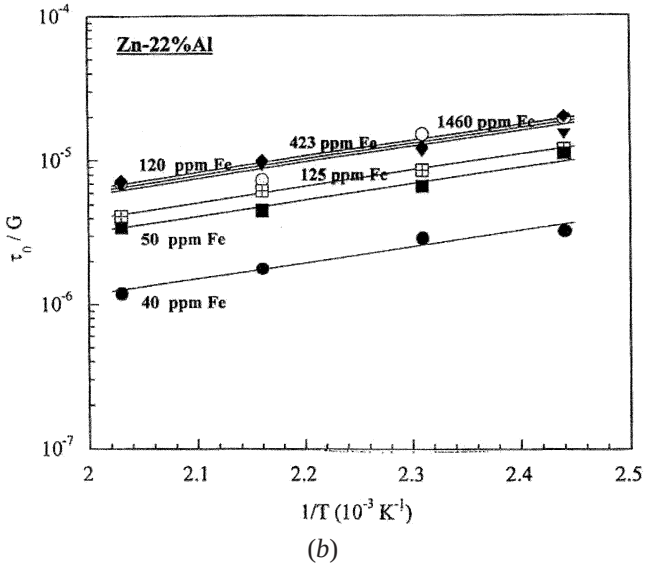

(*b*)

Fig. 9—(*a*) Determination of the threshold stress, τ_0, for superplastic flow in Zn-22 pct Al. Commercial purity Zn-22 pct Al and high-purity Zn-22 pct Al contain 180 and 6 ppm of impurities, respectively. Data were taken from Ref. 72. (*b*) A plot of the logarithm of τ_0/G as a function of $1/T$ for of Zn-22 pct Al grades having a grain size of 2.5 μm and containing 1460, 423, 125, 120, 50, and 40 ppm of Fe, respectively.

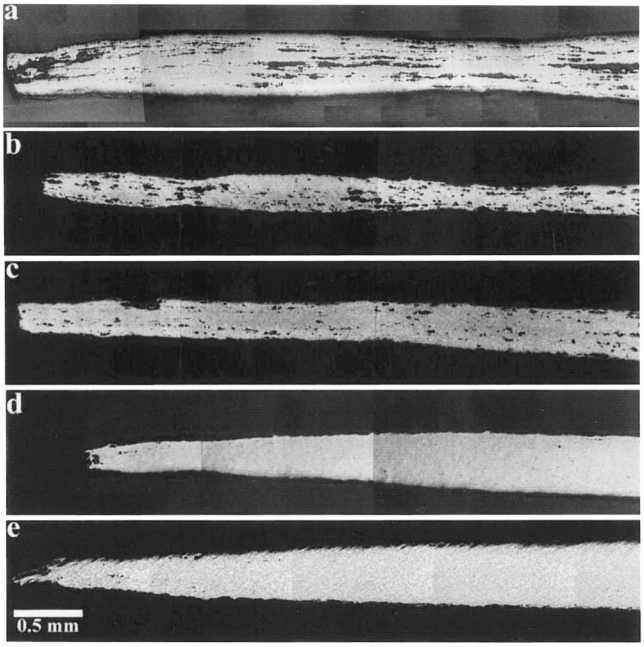

Fig. 10—Cavitation in different grades of Zn-22 pct Al tested at 473 K and an initial strain rate of 133×10^{-3}: (*a*) grade Fe with 1400 ppm Fe, (*b*) grade 1 with 180 ppm impurities, (*c*) grade 2 with 100 ppm impurities, (*d*) high-purity grade with 6 ppm impurities, and (*e*) grade Cu with 1300 ppm Cu.

variation in the average FαB domain size (D_α), as a function of annealing time (t_S), exhibits an initial short stage in which the increase is rapid, followed by a longer stage in which the increase becomes slow. The annealing curves shown in Figure 12 are similar in trend to those reported for the effect of solute additions on grain growth in zone-refined metals.[89] Consideration of the data of the figure shows the following trends: (1) grade HP (high-purity grade, 6 ppm of impurities) exhibits a much more drastic increase in D_α as compared to grades 1 and 2; (2) D_α in grade 1 (180 ppm of impurities) is always smaller than that in grade 2 (100 ppm of impurities); and (3) the data on grade Cu (1300 ppm), which does exhibit significant cavitation, fall very close to those on the high-purity grade of the alloy, while the data on grade Fe (1400), which exhibits significant cavitation, fall slightly below those on grade 1. These trends imply that the extent of impurity segregation is highest in grade Fe and lowest in grade HP, and that Cu, unlike Fe, has little or no tendency to segregate at boundaries. Such implications regarding the extent of segregation in the five grades are in agreement with the extent of cavitation, as shown in Figure 12. Also, as discussed elsewhere,[81] the aforementioned trends are consistent with the results of a quantitative analysis that is based on equations[90–93] and theories[94] developed for normal grain growth in metals and alloys. Also, the experimental data for each grade, when plotted as D_α against t on a logarithmic scale, can be represented reasonably well by a straight line whose slope is N. The form of this plot and the straight-line relationship between D_α and t are consistent with the following semiempirical equation proposed for normal grain growth in pure metals and alloys: $d = K t^N$, where d is the grain size, N is the growth exponent, and K is a function of temperature. Furthermore, the values of N determined for the five grades are in good agreement with the trend of the variation of N with the purity of a metal in a grain-size-growth experiment: decreasing the impurity content results in an increase in N (in very pure metals or at very high temperatures, N approaches the limiting value of 0.5 for a very-high-purity metal and at very high temperatures). For example, under similar solutionizing temperatures, N values follow the same order observed for D_α, *i.e.*, N highest in grade HP ($N = 0.36$), followed in order by grade Cu ($N = 0.33$), grade 2 ($N = 0.16$), grade 1 ($N = 0.12$), and, finally, grade Fe ($N = 0.11$).

In addition to providing indirect evidence for the occurrence of segregation at boundaries in Zn-22 pct Al, the presence of FαBs was utilized to explain the formation of cavity stringers in the alloy. This explanation[79] is based on three primary characteristics of FαBs. First, FαBs, unlike the fine microduplex structure in Zn-22 pct Al, are elongated rather than equiaxed (Figure 11). Accordingly, these boundaries would be resistant to both boundary sliding and rotation. By serving as obstacles to the sliding of either individual

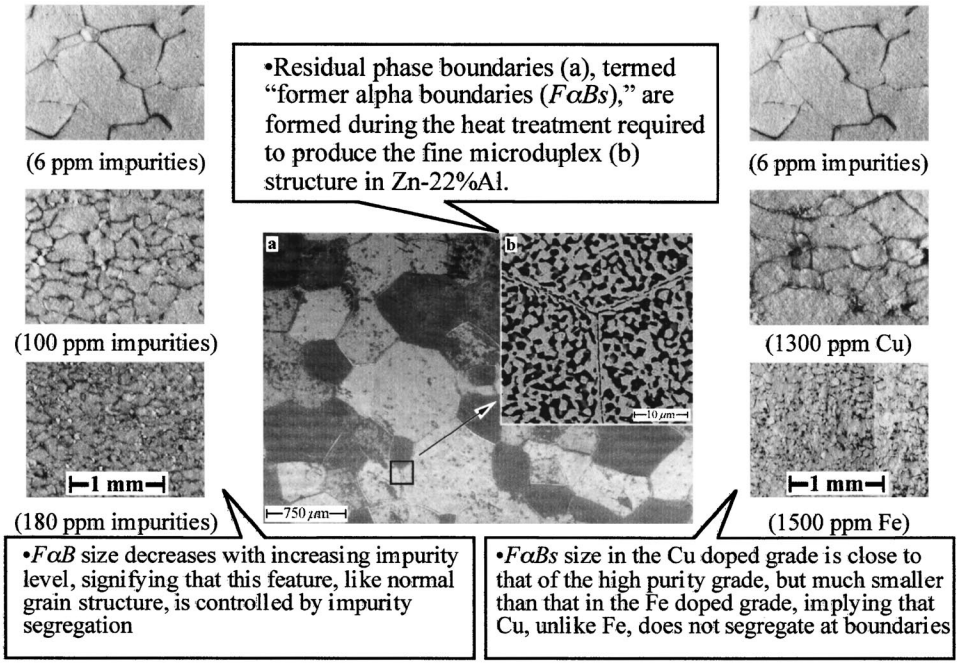

Fig. 11—The details of former alpha boundaries (*FαBs*) and their utilization in providing evidence for impurity segregation in Zn-22 pct Al.

grains of α and β or groups of these grains, FαBs would play a role similar to that of triple junctions or other discontinuities in the plane of the boundary. In the absence of accommodation by diffusion, boundary migration, and/or grain deformation, the stress concentrations at FαBs would be relieved by cavity nucleation. Second, segregation of impurities to FδBs is expected to result in nucleating cavities due to effects associated with the presence of excessive impurities at boundaries. Figure 13(a) shows the presence of cavities at FαBs. Third, in addition to serving as favorable cavity nucleation sites, recent microstructural observations have shown that, during superplastic deformation, FαBs change their orientation and become aligned with the tensile axis. This finding has not only rationalized the origin of cavity stringers in Zn-22 pct Al, as illustrated in Figure 13(b), but also provided a general explanation for cavity-stringer formation during superplastic flow.[79]

H. *Correspondence between the Effect of Impurities on the Sliding Contribution and the Effect of Impurities on Steady-State Creep Characteristics*

The view that GBS represents a major feature in micrograin superplasticity and is necessary for its occurrence was questioned by Mayo and Nix[95] on the basis of their results on superplastic deformation in torsion and indentation studies. These results have revealed two findings: (1) GBS occurs only in the initial stages of deformation (small strains), and (2) high values of strain-rate sensitivities (equivalent to low values of stress exponents) still characterize superplastic flow after GBS ceases. Because of these two findings and others related to substructural observations, including the formation of ligaments, Mayo and Nix[95] have concluded that GBS is not essential to the occurrence of superplasticity. However, Gifkins[96] and Valiev and Langdon[64] have argued that GBS plays a central role during superplastic flow. This argument is based on the following considerations: (1) GBS occurs at all strains (small and large) in region II, (2) the contribution of GBS to total strain is more significant in region II than in regions I and III, and (3) GBS is more difficult in torsion than in tension.

The preceding discussion demonstrates that impurities influence steady-state superplastic behavior at low stresses. This finding has been attributed to boundary segregation. On the basis of this interpretation, a correlation between boundary sliding behavior and impurities is expected to exist if sliding is an integral feature of superplasticity. Three studies, which were cited earlier,[38,39,40] were conducted to explore this expectation under the condition of small strains (20 to 30 pct). The first study[38] examined the effect of the total impurity content on boundary sliding in Zn-22 pct Al, the second study[39] focused on the effect of Cd on the sliding behavior of Pb-62 pct Sn, and the third study[40] dealt with the effect of Fe and Cu on the sliding behavior of Zn-22 pct Al. The results of these three studies have demonstrated that the effect of impurity type and level on the boundary-sliding contribution corresponds well with the effect of impurity level on steady-state creep characteristics and cavitation. Figure 14 illustrates this finding for impurity type (Cu and Fe). This correspondence indicates that at elongations of 20 to 30 pct, boundary sliding is an important feature of the deformation process that controls steady-state superplastic flow. Despite this finding, further studies are needed to investigate the effect of impurities on the contribution of boundary sliding to the total strain in Pb-62 pct Sn and Zn-22 pct Al at large strains ($>$20 pct). The data of such studies can be used to clarify the issue of whether the characteristics of boundary sliding reflect those of steady-state superplastic flow at all strains (small and large).

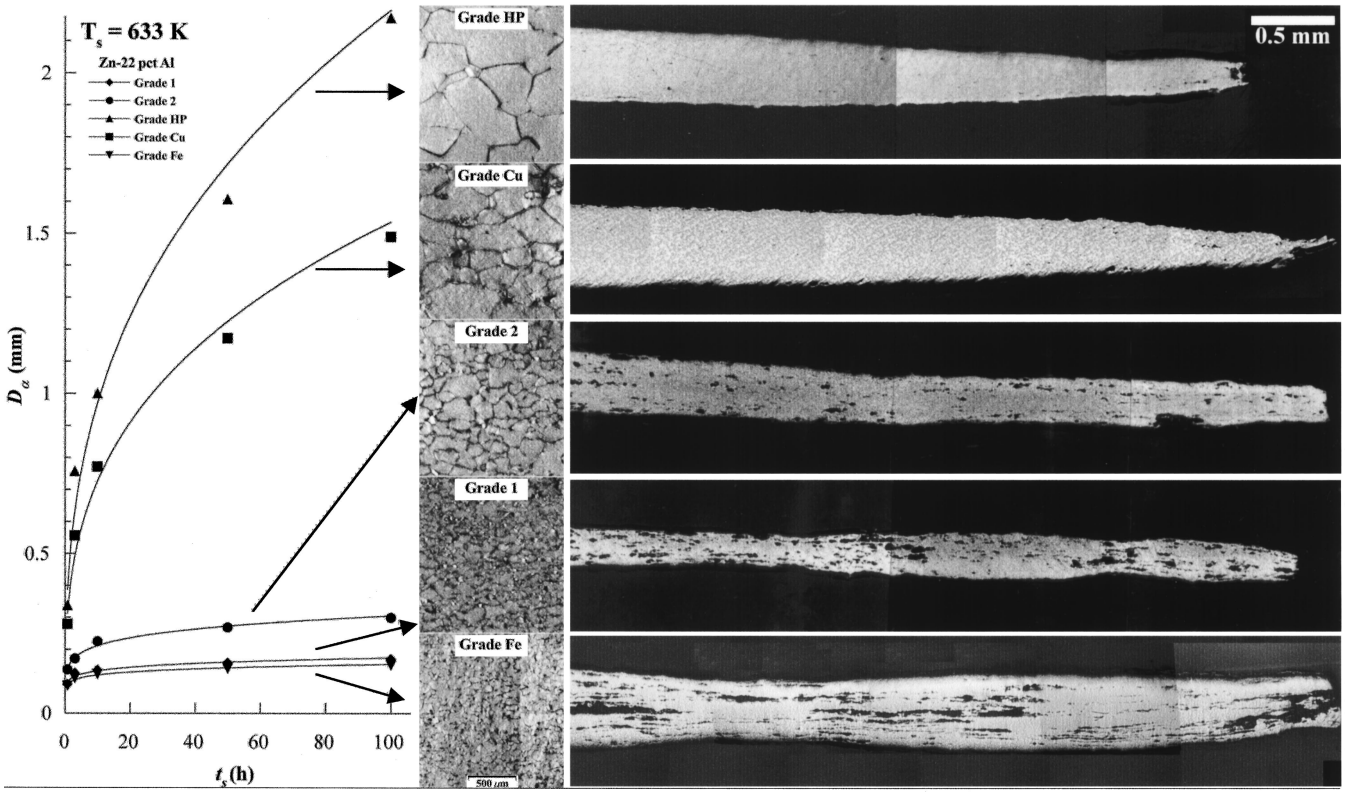

Fig. 12—The annealing curves for several grades of Zn-22 pct Al. The representative micrographs show (*a*) the former alpha boundary (*FαB*) domain size after annealing for 7 h and (*b*) the extent of cavitation in each grade.

III. HARPER–DORN CREEP

Detailed studies on the creep behavior of polycrystalline materials at very low stresses are of scientific and practical significance. From a scientific point of view, data obtained from such studies are critical to the characterization of creep behavior in terms of deformation mechanisms. From a practical point of view, information inferred from such studies is useful not only because of its relevance to the prediction of geological deformation but also because of its relevance to many design considerations.

A. *Nabarro–Herring Creep*

Early theoretical considerations[4,5] have indicated that the creep behavior of polycrystalline materials in the limit of high temperatures and low stresses may not be controlled by dislocation movement, but rather by the stress-directed diffusion of vacancies through the lattice. This mode of deformation, known as Nabarro–Herring creep, is one of the high-temperature deformation mechanisms that have been modeled on a firm theoretical basis. The creep rate for Nabarro–Herring creep is given by[4,5,41]

$$\frac{\dot{\gamma} kT}{DG\mathbf{b}} = B\left(\frac{\mathbf{b}}{d}\right)^2 \left(\frac{\tau}{G}\right) \qquad [4]$$

The dimensionless constant, *B*, depends on the geometry of the grains and on the stress distribution within grains. Over the years, the theory of Nabarro–Herring creep was modified[97] to incorporate features (such as the inability of boundaries to perfect sources and sinks for vacancies) that were not considered in the original development and which were found necessary to account for some deviation from the prediction. Despite these modifications, the grain-size sensitivity of the Nabarro–Herring process remains a testing parameter for the correlation between theory and experiment. For example, if a single crystal is creep tested at a very low stress in the Nabarro–Herring domain, the resultant creep rate is expected to be negligible.

B. *Harper–Dorn Creep*

A creep investigation by Harper and Dorn[15,16] on large-grained aluminum specimens (grain size = 3.3 mm) at very low stresses and temperatures near the melting point, where Nabarro–Herring creep is expected to occur, revealed a new Newtonian creep behavior whose rates are more than two orders of magnitude faster than those predicted by Eq. [4] (Figure 15). This enhancement of creep rates in large-grained Al, along with several other characteristics[15,16] such as the agreement between single and polycrystalline creep rates, led to the conclusion that the low-stress creep behavior of Al was controlled by a dislocation process and not by Nabarro–Herring creep.[4,5]

Over the past three decades, Harper-Dorn creep has received considerable attention. First, additional experiment data were obtained on Al and other materials (for review, see References 98 through 100). These data appear to suggest that Harper–Dorn creep is a general type of creep behavior which dominates at low stresses and large grain sizes. Second, suggestions were made to account for the origin of strain[101,102,103] during Harper–Dorn creep.

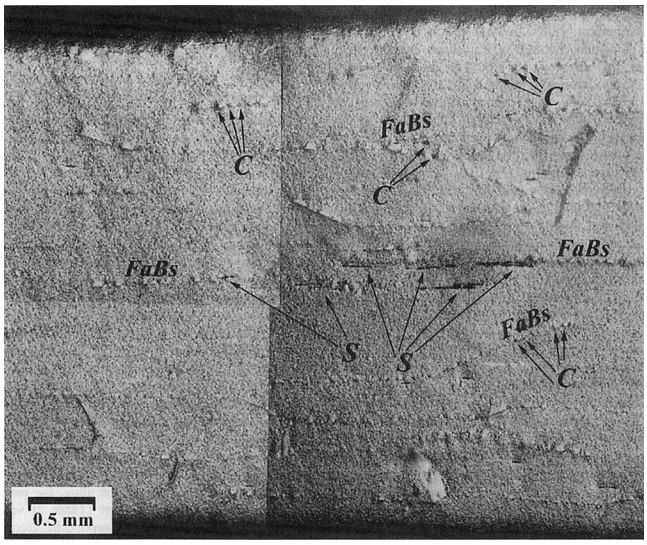

(*a*)

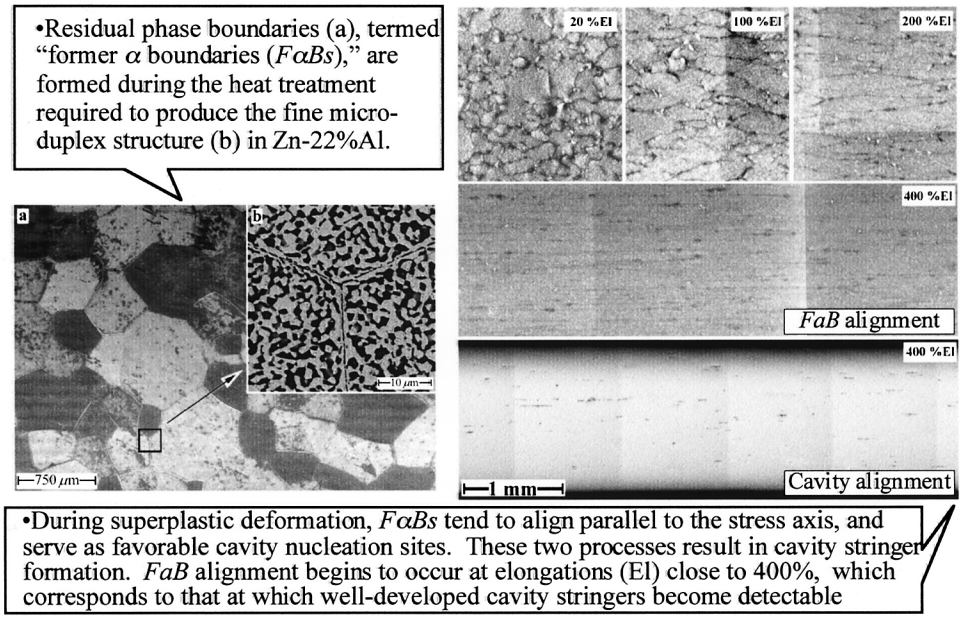

(*b*)

Fig. 13—(*a*) Nucleation of cavities at former alpha boundaries (*FαBs*). (*b*) Correlation between the characteristics of former alpha boundaries, *FαBs* (the rotation of the boundaries, during deformation and their aligned with the tensile axis), and the formation of cavity stringers in Zn-22 pct Al.; %El refers to the percentage elongation.

Third, sources for dislocation multiplication were speculated. These sources are a climb-diffusion–controlled process,[104] cross slip,[101] and surface dislocation sources.[105] Furthermore, it was suggested[106] that the value of the dislocation density in Harper–Dorn creep is controlled by the Peierls stress of the material and not by applied stress. Finally, investigators put forward a number of deformation processes[16,100,102–104,106–113] that are capable of accounting for the characteristics of Harper–Dorn creep, such as the Newtonian nature ($n = 1$), the activation energy ($Q = Q_d$), the grain-size insensitivity, and the values of the creep rates. These deformation processes were reviewed elsewhere.[98,99,100]

C. *Issues Related to Harper–Dorn Creep*

Despite the aforementioned results and their impact on fundamental creep knowledge, several issues regarding Harper–Dorn Creep have remained unclear until recently. In the next section, some of these issues are identified, and recent results that have addressed them are briefly described.

1. *The nature of Harper–Dorn creep*

The creep experiments conducted on Al at very low stresses in the Harper and Dorn domain[15,16,100,104,114] are characterized by two primary features: (1) the creep rates were of the order of 8×10^{-8} to 3×10^{-9} s^{-1}, and (2) the creep tests were conducted for periods of time less than 200

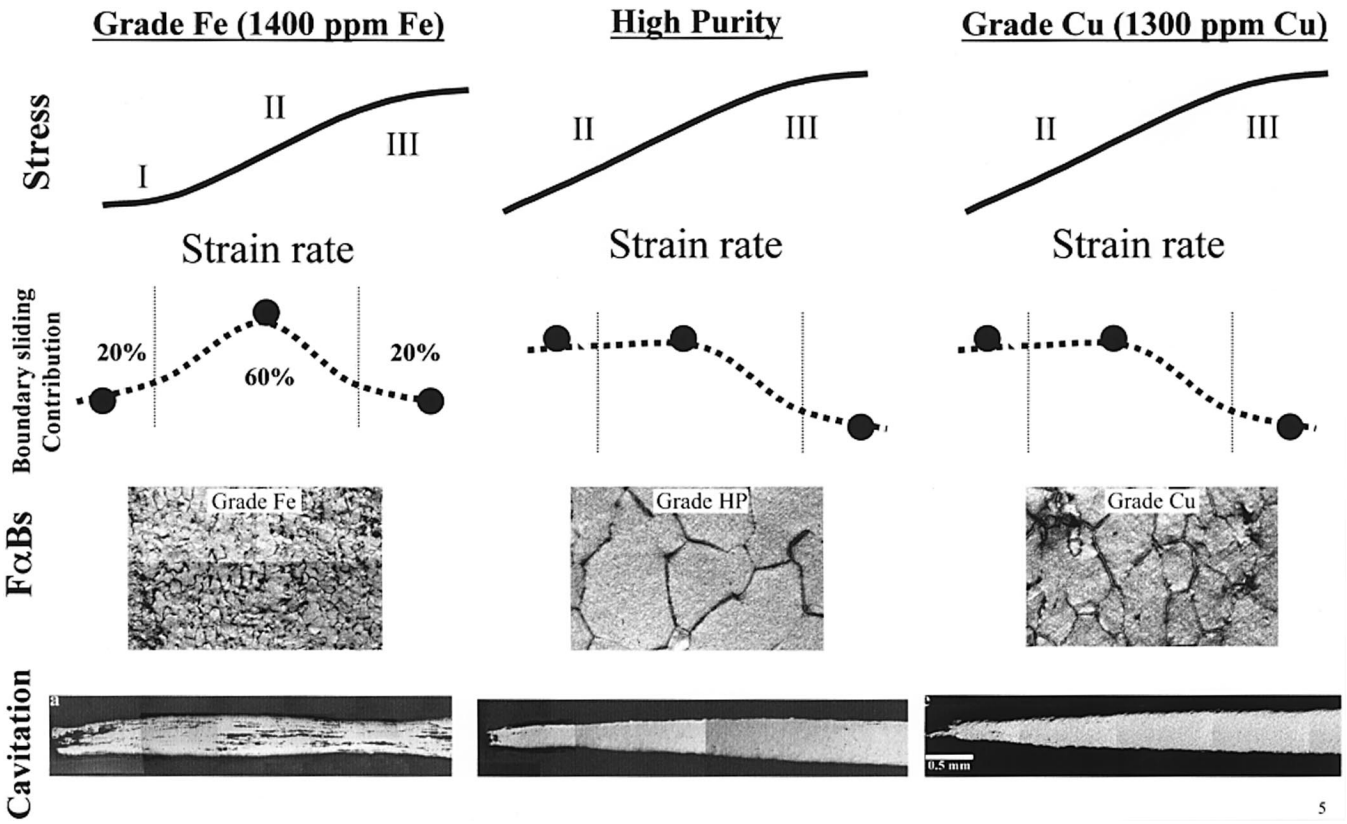

Fig. 14—Correspondence between sliding behavior (the contribution of boundary sliding to the total strain) and superplastic behavior in Zn-22 pct Al (region I at low strain rates and cavitation).

hours. As a result, the amount of creep strain measured did not exceed 0.01. With such small strains, it is difficult to ascertain whether Harp–Dorn creep is a genuine creep process or a transient phenomenon. This issue was addressed by Mohamed and Ginter,[101] who conducted long-term creep tests in which emphasis was placed on the amount of creep strain measured during the test and not on its duration. The results of Mohamed and Ginter have demonstrated[101] that Harper–Dorn creep arises from a genuine creep process that results in large creep strains (greater than 10 pct). In addition, the results have led to the conclusion that the occurrence of Harper–Dorn in Al requires the presence of a certain substructural characteristic related to the initial dislocation density (Section 3–C–III).

2. *The shape of creep curve*

Earlier data on Harper–Dorn creep in Al[15,16,100,104,114] showed that the creep curve exhibited a normal primary stage followed by a steady-state stage. However, as mentioned previously, the strain allowed in creep tests is too small to make a definitive conclusion with respect to the characteristics and shape of the creep curve. Very recently, Ginter *et al.*[116] closely examined the shape of the creep curve of Al that exhibited the accelerated creep rates associated with Harper–Dorn creep. Such an examination was performed by conducting large strain–long term tests and by carefully monitoring creep strain as a function of time. The results[116] have shown that after a creep strain of about 2 pct, the creep curve is not smooth, and there are periodic accelerations over the curve (Figure 16). It has also been demonstrated[116] that these accelerations represent genuine behavior that may have been overlooked in an earlier investigation,[101] which involved long-term creep tests, as a result of the scale used in constructing the creep curve.

3. *The reproducibility of Harper–Dorn in Al*

There is conflicting evidence regarding the occurrence of Harper–Dorn creep in coarse-grained materials when creep tested at very low stresses. Perhaps the most typical example of such a conflict is provided by the results on Al. On the one hand, the results of the short-term creep tests of Harper and Dorn[15] ($t < 200$ hours and creep strain < 0.1) are in agreement with those of three subsequent independent creep investigations,[102,104,115] which were also conducted under similar conditions (short-term tests resulting in small strains). In the first investigation, Barrett *et al.*[104] tested tensile specimens of both single and polycrystalline Al. The second investigation, using double-shear specimens of both single and polycrystalline al, was conduced by Mohamed *et al.*[115] The third investigation was performed by Lee and Ardell,[102] who tested Al single specimens in compression. On the other hand, Burton reported[117] that Harper–Dorn creep in coarse-grained Al could not be reproduced under the conditions of his experiment, although he was able to observe Nabarro–Herring creep in fine-grained thin foils of Al. In addition, on the basis of their low-stress creep data on Al, Blum and Maier[118] have very recently questioned the existence of Harper–Dorn creep.

The creep results reported by Ginter and Mohamed[101] and by Ginter *et al.* and Mohamed *et al.*[116] for Al have

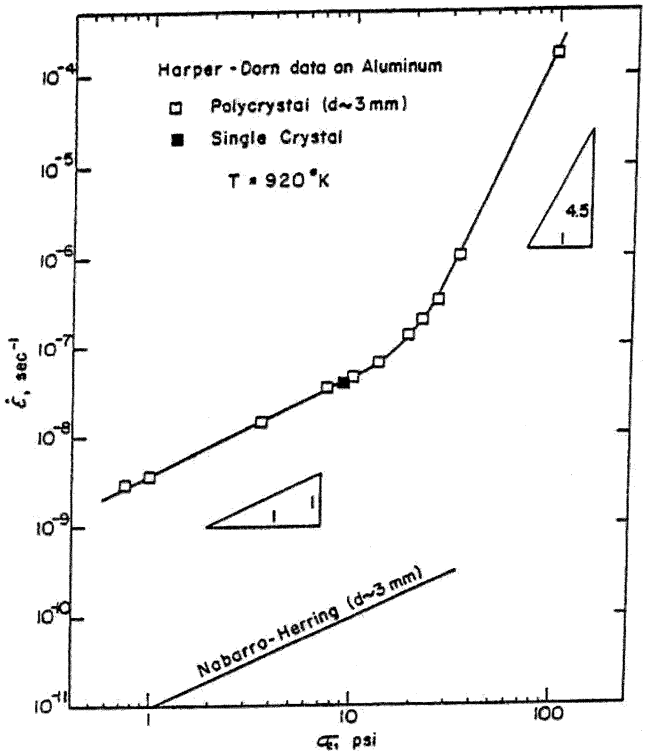

Fig. 15—Original creep data reported for Al by Harper and Dorn[15] at low stresses. The data are plotted as creep rate against effective stress on a logarithmic scale. Shown is the prediction of the equation representing Nabarro–Herring creep.[4,5]

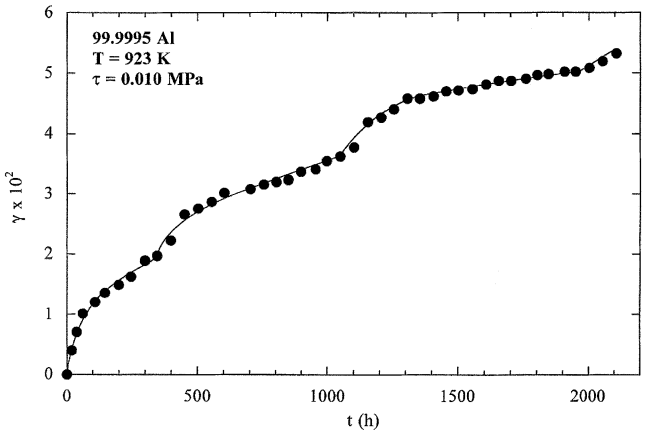

Fig. 16—Shear strain *vs* time for 99.9995 Al ($T = 923$ K; $\tau = 0.01$ MPa). The creep curve exhibits regular, periodic accelerations.

presented a possible explanation for the dichotomy in the creep behavior of this metal at low stresses. These results[101,116] have shown that the Harper–Dorn process does not always control the creep behavior of coarse-grained Al at very low stresses, and that such a process occurs at low stresses under two conditions: (1) the dislocation density in the annealed samples is low (10^3 to 3×10^4 cm^{-2}), and (2) the purity level is very high. According to the data of Mohamed and Ginter,[101] Harper–Dorn creep did not occur in Al samples in which the dislocation density was high (10^6 cm^{-2}; Figure 17(a)) and whose purity was 99.99; on the other hand, Al samples of high purity (99.9995) and low

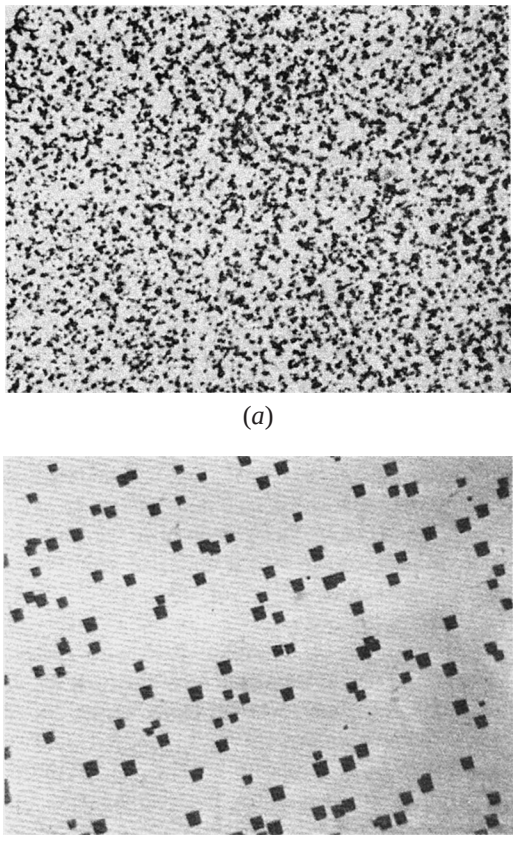

(*a*)

(*b*)

Fig. 17—Etch-pit photographs of two Al grades after annealing for 50 h at 926 K: (*a*) 99.99Al (dislocation density $\sim 2 \times 10^{-6}$ cm^{-2}), magnification 145 times; and (*b*) 99.9995Al (dislocation density $\sim 2 \times 10^{-4}$ cm^{-2}), magnification 55 times.

dislocation density ($\sim 10^6$; cm^{-2}; Figure 17(b)) exhibited Harper–Dorn creep.

In addition, consideration of the results of Ginter *et al.*[116] and those of Mohamed and Ginter[101] leads to the conclusion that high purity, like a large grain size, is a necessary but not sufficient condition. This conclusion is based on the finding[101] that 99.9995 Al, like 99.99 Al, exhibited negligible creep rates in the Harper–Dorn region when the initial dislocation density was high (4×10^6 cm^{-2}).

4. *The details of creep microstructure during Harper–Dorn creep*

Through the use of Laue X-ray, Harper and Dorn[15] reported no subgrain formation in Al. This observation agreed with the etch-pit results subsequently obtained by Harper *et al.*[16] On the other hand, Barrett *et al.*,[104] using etch pitting, Laue X-ray back reflection, and Lang topography, noted the formation of subgrains. It was suggested that the failure to observe subgrains during Harper–Dorn creep might be the result of one or a combination of three possibilities: (1) subgrains might have annealed out from samples tested due to cooling slowly without loads, (2) creep strains were not sufficiently large to allow the full development of subgrains, and (3) the average subgrain sizes might have approached or exceeded the grain size of the samples tested in the stress range of Harper–Dorn creep.

In order to address the issue of subgrain formation, Ginter and Mohamed[119] conducted experiments under conditions

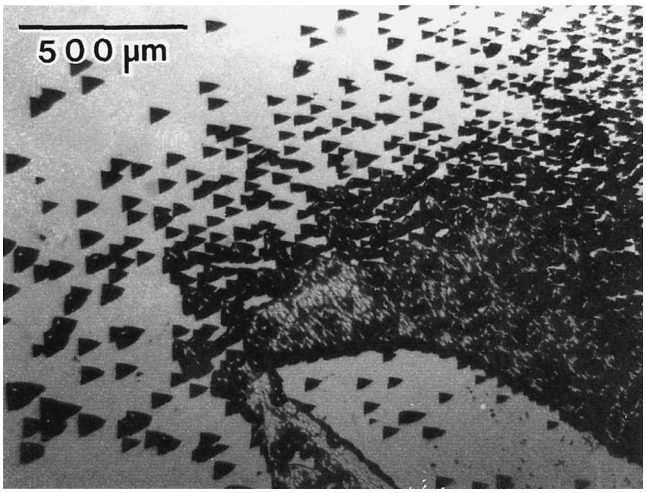

(*a*)

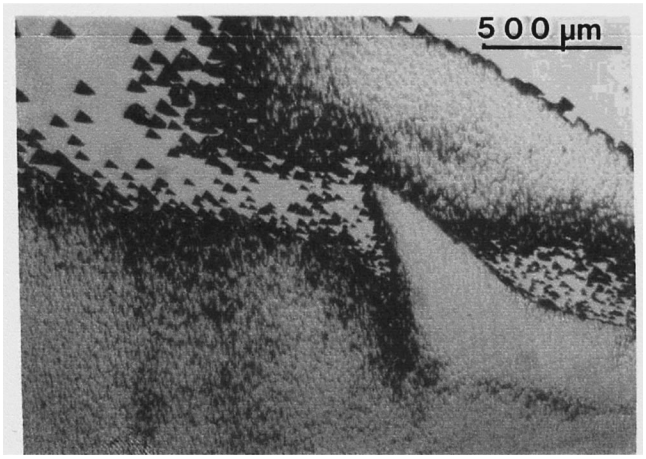

(*b*)

Fig. 18—Etch-pit photographs of 99.995 Al deformed in shear: (*a*) 923 K and 0.025 MPa, showing the nucleation of new grains; and (*b*) 923 K and 0.623 MPa, showing regions of high and low dislocation densities and the wavy nature of boundaries.

that eliminated the three aforementioned possibilities. In these experiments, Al samples (99.9995 purity and low annealed dislocation densities), in which the average grain size was 9 mm and which exhibited accelerated creep rates associated with Harper–Dorn creep, were deformed to strains larger than 10 pct and then were quenched rapidly under load. According to the equation relating subgrain size to stress,[41,49,51] if subgrains were developed during Harper–Dorn creep, their average size at 0.025 MPa would be approximately 2 mm, a value which is much smaller than the average grain size of 9 mm. The results of the previous experiments have shown the absence of a well-defined subgrain network. In addition, the results have indicated the presence of the following features: (1) new grains nucleated near the free surface (Figure 18(a)), (2) high gradients of the dislocation density across migrating grain boundaries (Figure 18(b)), (3) wavy boundaries with high and low dislocation densities on opposite sides of the boundary, and (4) localized regions of very high dislocation density.

Mohamed and Ginter[101] and Ginter *et al.*[116] also conducted experiments on Al (99.99 purity and high annealed dislocation densities) which did not exhibit the accelerated

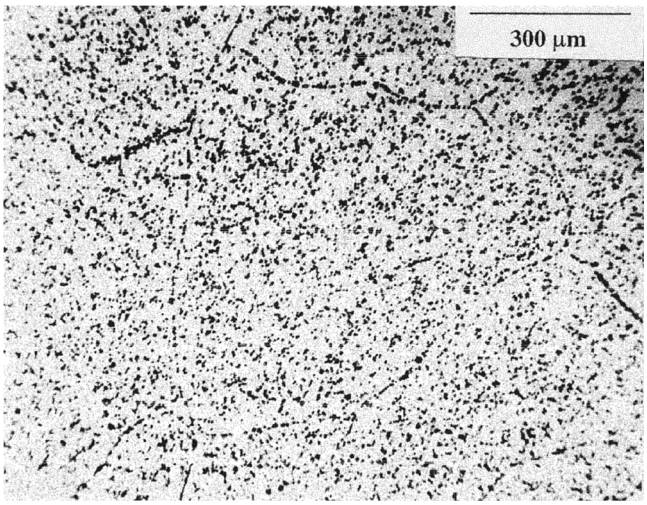

Fig. 19—Etch-pit photograph of 99.99 Al after deformation at 923 K and 0.04 MPa, showing the presence of subgrain structure. Data taken from Ref. 116.

creep rates characterizing Harper–Dorn creep. Their etch-pit results showed that at high stresses, an extensive, regular array of subgrains and well-developed subboundaries were present over the entire gage, and that at low stresses typical of those associated with Harper–Dorn creep, etch pits defined very large subgrains or appeared as isolated long sub-boundaries Figure 19. These features sharply contrast with those characterizing the behavior that is noted in high-purity Al (99.999) samples whose initial dislocation densities ($\sim 10^4$ cm^{-2}) were low and which exhibited accelerated creep rates.

5. *The stress dependence of Harper–Dorn creep*

One of the primary characteristics of Harper–Dorn creep is that the creep rate is linearly related to stress (Newtonian behavior). However, this characteristic was determined for Al from short-term tests that involved strains less than 0.01. Weertman[120] argued that the Newtonian behavior noted in samples crept for small strains under very low stresses may not represent the true behavior for large strains, but may be the result of two conditions: (1) a very insignificant variation in the dislocation density over a limited amount of strain, and (2) a linear dependence of the dislocation velocity on stress. This argument has raised the following issue: whether the Newtonian nature of Harper–Dorn creep represents a genuine characteristic or is a consequence of measurements made at small strains.

The aforementioned issue was very recently addressed by Ginter *et al.*,[116] who performed long-term creep experiments that involved large strains. While the results of these experiments have verified the Newtonian nature of Harper–Dorn creep at small strains (less than 0.01), they have indicated that under the condition of large strains (more than 0.1), the stress exponent is more than 2 (Figure 20). It has also been shown that when short-term creep curves were constructed by using the data on 99.9995 Al and by plotting creep strain *vs* time for a total time of only 200 hours (the maximum duration of previous investigations on Al), the data can be erroneously divided into two stages: a primary stage, in which the creep rates decrease with time, and a secondary stage, in which the creep rate is constant.

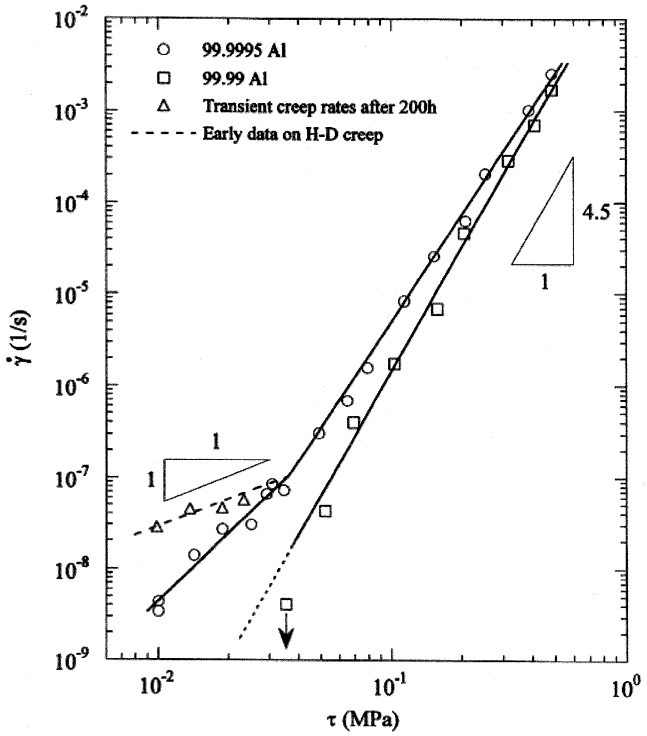

Fig. 20—Shear strain rate *vs* applied shear stress on a logarithmic for 99.99Al and 99.995Al tested at 923 K. Data taken from Ref. 116.

6. *The nature of the restoration mechanism in Al during Harper–Dorn*

Several deformation processes proposed to explain Harper–Dorn creep implicitly or explicitly incorporate dynamic recovery, through dislocation annihilation, as the restoration process. However, according to the results of Ginter *et al.*,[116] the mechanical and substructural characteristics of 99.9995 Al, which exhibit accelerated creep typical of Harper–Dorn creep, agree well with those of dynamic recrystallization as the dominant restoration mechanism during the creep of 99.9995 Al. These characteristics include the nucleation of new grains, the absence of a regular array of subgrains, the presence of wavy boundaries and localized regions of very high dislocation density, and the occurrence of periodic accelerations over the entire curve. It is well documented that during mechanical testing, dynamic crystallization in metals such as Cu, Ni, and Pb is generally manifested by periodic accelerations in the creep rate on the strain-time plots at constant stresses. For example, in his study on pure Pb, Gifkins[121] reported similar accelerations in the creep curve obtained as a result of deformation in tension (Figure 21). Gifkins suggested[121] that these periodic accelerations were the result of the occurrence of transient creep in the recrystallized regions.

Finally, it was reported that during Harper–Dorn creep, the dislocation density is low and independent of stress. This characteristic provided the basis for most of the models proposed for Harper–Dorn creep. Ginter *et al.*[116] did not report measurements of dislocation density as a function of stress, but their micrographs showed a wide variation of dislocation densities within the section of the specimen, localized regions of both extremely high and low dislocation regions, and new grains. These features are expected to have a strong influence on masking the true stress dependence of

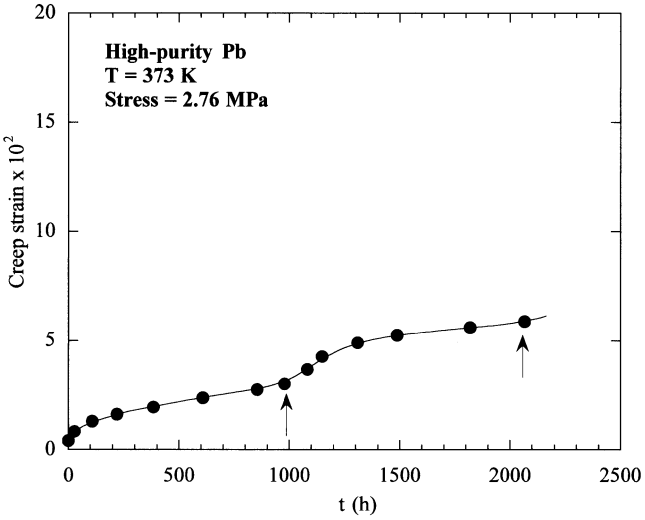

Fig. 21—Creep curve for high-purity Pb deformed in tension showing accelerated creep associated with dynamic recrystallization. Data taken from Ref. 121.

dislocation density, especially in view of the fact that dynamic recrystallization is a continuous process. Also, as a result of the occurrence of dynamic recrystallization, which, as mentioned previously, is the source of the accelerated creep rate associated with Harper–Dorn creep, two possibilities may be considered. First, it is quite possible that once a grain is nucleated, the boundary separating the high-dislocation-density region and the low-dislocation-density region sweeps across the gage, resulting in an area of a low, random dislocation density. Second, it is quite possible that only one boundary may sweep a significant portion of the gage before a second grain is nucleated. This possibility may lead to the observation that when the specimen is sectioned, a low dislocation density, whose value is comparable to that of the annealed sample, exists in this portion of the section.

IV. CONCLUSIONS

1. For micrograined superplastic alloys ($d < 10$ μm) such as Zn-22 pct Al, which display superplastic behavior (tensile elongation > 300 pct) and whose creep behavior often exhibits a sigmoidal relationship between the stress and strain rate, the low-stress region of such a relationship (region I) as well as cavitation are absent when the impurity level becomes less than 6 ppm. By contrast, when impurities are present, region I becomes well defined, a threshold stress for superplastic behavior exists, and cavities tend to align along the tensile axis (cavity stringers). These effects, and others, are most probably a consequence of impurity segregation at boundaries.
2. For coarse-grained Al ($d > 1$ mm), the accelerated creep rates associated with Harper–Dorn creep are observed at very low stresses only when (1) the purity of samples is very high (99.999), and (2) the initial dislocation densities are low ($\sim 10^4$ cm^{-2}). These two conditions favor dynamic recrystallization as the dominant restoration mechanism in Al. In particular, a high purity leads to high boundary mobility. Consistent with this conclusion

is the observation that as the purity level of Al increases from 99.99 to 99.999, the creep microstructure changes from that associated with dynamic recovery (subgrain formation) to that characterizing dynamic recrystallization (the nucleation of new grains, the absence of a regular array of subgrains, and the presence of wavy boundaries).

ACKNOWLEDGMENTS

This work was supported by the National Science Foundation under Grant No. DMR-9810422.

REFERENCES

1. H. Gleiter and B. Chalmers: *Progr. Mater. Sci.*, 1972, vol. 16.
2. H.C. Chang and N.J. Grant: *Trans: Trans. AIME.*, 1956, vol. 206, pp. 544-51.
3. H. Riedel: in *Fracture at High Temperatures*, B. Ilschner and N. Grant, eds., MRE Springer-Verlag, New York, NY 1986, pp. 116-47.
4. F.R.N. Nabarro: *Report on a Conference on Strength of Solids*, Physical Society, London, 1948, p. 75.
5. C. Herring: *J. Appl. Phys.*, 1950, vol. 21, pp. 437-45.
6. R.L. Coble: *J. Appl. Phys.*, 1964, vol. 34, pp. 1679-82.
7. C.J. McMahon: *ASTM STP*, 1968, vol. 407, pp. 127-67.
8. D.P. Pope and D.S. Wilkinson: in *Recent Advances in Creep and Fracture of Engineering Materials and Structures*, B. Wilshire and D.R.J. Owen, eds., Pineridge Press, Swansea, 1981, pp. 351-544.
9. C.T. Liu, C.L. White, C.C. Koch, and E.H. Lee: in *High Temperature Materials Chemistry—II*, Z.A. Munir and D. Cubicciotti, eds., The Electrochemical Society, Pennington, NJ, 1983, pp. 32-41.
10. T. Taylor and R.L. Edgar: *Metall. Trans.*, 1971, vol. 2, pp. 883-39.
11. A.K. Mukherjee: *Ann. Rev. Mater. Sci.*, 1979, vol. 9, pp. 191-217.
12. R.C. Gifkins: in *Superplastic Forming of Structural Alloys*, N.E. Paton and C.H. Hamilton, eds., TMS-AIME, San Diego, CA, 1982, pp. 2-26.
13. O.D. Sherby and J. Wadsworth: *Progr. Mater. Sci.*, 1989, vol. 33, pp. 169-221.
14. H. Chokshi, A.K. Mukherjee, and T.G. Langdon: *Mater. Sci. Eng. Rep.*, 1993, vol. R10, pp. 237-74.
15. J. Harper and J.E. Dorn: *Acta Metall.*, 1957, vol. 5, pp. 654-65.
16. J. Harper, L.A. Shepard, and J.E. Dorn: *Acta Metall.*, 1958, vol. 6, pp. 509-18.
17. W.A. Backofen, I.R. Turner, and D.H. Avery: *Trans. ASM*, 1964, vol. 57, pp. 980-16.
18. T.H. Alden: *Acta Metall.*, 1967, vol. 15, pp. 469-79.
19. W.B. Morrison: *Trans. ASM*, 1968, vol. 61, pp. 423-34.
20. J. Hedworth and M.J. Stowell: *J. Mater. Sci.*, 1971, vol. 6, pp. 1061-69.
21. G.B. Gibbs: *Phil. Mag.*, 1966, vol. 13, pp. 317-29.
22. A. Arieli and A. Rosen: *Scripta Metall.*, 1976, vol. 10, pp. 471-75.
23. E.W. Hart: *Acta Metall.*, 1970, vol. 18, pp. 599-610.
24. P.K. Chaudhury and F.A. Mohamed: *Acta Metall.*, 1988, vol. 36, pp. 1099-1110.
25. F.A. Mohamed and T.G. Langdon: *J. Mater. Sci.*, 1982, vol. 17, pp. 1925-29.
26. H.I. Huang, D. Sherby, and J.E. Dorn: *Trans. TMS-AIME*, 1956, vol. 206, pp. 1385-88.
27. P. Chaudhari: *Acta Metall.*, 1967, vol. 15, pp. 1777-86.
28. F.A. Mohamed and T.G. Langdon, *Phys. Status Solidi (a)*, 1976, vol. 33, pp. 375-81.
29. D. Lee: *Acta Metall.*, 1969, vol. 17, pp. 1057-69.
30. O.A. Kaibyshev, R.Z. Valeiv, and V.V. Astamin: *Phys. Status. Solidi*, 1976, vol. 35, pp. 403-13.
31. I.I. Novikov, V.K. Portnoy, and T.E. Terentieva: *Acta Metall.*, 1977, vol. 25, pp. 1139-49.
32. N. Furushiro and S. Hori: *Scripta Metall.*, 1979, vol. 13, pp. 653-56.
33. R.B. Vastava and T.G. Langdon: *Acta Metall.*, 1979, vol. 27, pp. 251-57.
34. Z.-R. Lin, A.H. Chokshi, and T.G. Langdon: *J. Mater. Sci.*, 1988, vol. 23, pp. 2712-22.
35. P. Shariat, R.B. Vastava, and T.G. Langdon: *Acta Metall.*, 1982, vol. 30, pp. 285-96.
36. R.C. Gifkins: *Metal Forum*, 1991, vol. 15, pp. 82-94
37. K.T. Park, S. Yan, and F.A. Mohamed: *Phil. Mag.*, 1995, vol. 72A, pp. 891-903.
38. K. Duong and F.A. Mohamed: *Acta Mater.*, 1998, vol. 46, pp. 4571-86.
39. K. Duong and F.A. Mohamed: *Phil. Mag.*, 1999, vol. 80A, pp. 2721-35.
40. K. Duong and F.A. Mohamed: *Metall. Mater. Trans. A*, 2001, vol. 32A, pp. 103-13.
41. J.E. Bird, A.K. Mukherjee, and J.E. Dorn: in *Quantitative Relation between Properties and Microstructure*, D.G. Brandon and A. Rosen, eds., Israel University Press, Jerusalem, 1969, pp. 255-342.
42. F.A. Mohamed and T.G. Langdon: *Acta. Metall.*, 1975, vol. 23, pp. 117-24.
43. F.A. Mohamed, S.A. Shei, and T.G. Langdon: *Acta. Metall.*, 1975, vol. 23, pp. 1443-50.
44. F.A. Mohamed and T.G. Langdon: *Phil. Mag.*, 1975, vol. 32, pp. 697-709.
45. S.H. Vale, D.J. Eastgate, and P.M. Hazzledine: *Scripta Metall.*, 1979, vol. 13, pp. 1157-62.
46. D.W. Livesey and N. Ridley: *Scripta Metall.*, 1982, vol. 16, pp. 165-68.
47. S.A. Shei and T.G. Langdon: *Acta Metall.*, 1978, vol. 26, pp. 638-46.
48. A.H. Chokshi and T.G. Langdon: *Metall. Trans. A*, 1988, vol. 19A, pp. 2487-96.
49. F.A. Mohamed and T.J. Ginter: *J. Mater. Sci.*, 1982, vol. 17, pp. 2007-12.
50. F.A. Mohamed and T.G. Langdon: *Scripta Met.*, 1976, vol. 10, pp. 759-62.
51. M.S. Soliman, T.J. Ginter, and F.A. Mohamed: *Phil. Mag.*, 1993, vol. A48, p. 63.
52. B.P. Kashyap, A. Arieli, and A.K. Mukherjee: *J. Mater. Sci.*, 1985, vol. 28, pp. 2661-86.
53. A. Vevecka and T.G. Langdon: *Mater. Sci.*, 1994, vol. A187, pp. 161-65.
54. M.F. Ashby and R.A. Verrall: *Acta Metall.*, 1973, vol. 21, pp. 149-63.
55. A. Ball and M.M. Hutchison: *Met. Sci. J.*, 1969, vol. 3, pp. 1-7.
56. A.K. Mukherjee: *Mater. Sci. Eng.*, 1971, vol. 8, pp. 83-89.
57. R.C. Gifkins: *Metall. Trans. A*, 1976, vol. 7A, pp. 1225-32.
58. J.H. Gittus: *Trans. ASME, H. J. Eng. Mater. Technol.*, 1977, vol. 99, pp. 244-51.
59. A. Arieli and A.K. Mukherjee: *Mater. Sci. Eng.*, 1980, vol. 45, pp. 61-70.
60. V. Paidar and S. Takeuchi: *Acta. Metall. Mater.*, 1992, vol. 40, pp. 1773-82.
61. P.K. Chaudhury, K.T. Park, and F.A. Mohamed: *Metall. Mater. Trans. A*, 1994, vol. A25, pp. 2391-2401.
62. S. Yan, J.C. Earthman, and F.A. Mohamed: *Phil. Mag. A*, 1994, vol. 69, pp. 1017-38.
63. R.Z. Valiev and O.A. Kaibyshev: *Acta Metall.*, 1983, vol. 31, pp. 2121-28.
64. R.Z. Valiev and T.G. Langdon: *Acta Metall. Mater.*, 1993, vol. 41, pp. 949-54.
65. T.G. Langdon: *Mater. Sci. Eng.*, 1994, vol. A174, pp. 225-30.
66. R.H. Johnson: *Met. Rev.*, 1970, vol. 15, pp. 115-34.
67. B. Burton: *Scripta Metall.*, 1971, vol. 5, pp. 669-72.
68. G. Rai and N.J. Grant: *Metall. Trans. A*, 1975, vol. 6A, pp. 385-90.
69. A. Arieli and A.K. Mukherjee: *Scripta Metall.*, 1979, vol. 13, pp. 331-38.
70. M.L. Vaidy, K.L. Murty, and J.E. Dorn: *Acta Metall.*, 1973, vol. 21, pp. 1615-23.
71. S.C. Misro and A.K. Mukherjee: *Rate Processes in Plastic Deformation*, Proc. John E. Dorn Memorial Symp., J.C.M. Li and A.K. Mukherjee, eds., ASM, Cleveland, OH, 1975, pp. 434-58.
72. P.K. Chaudhury, V. Sivaramakrishnan, and F.A. Mohamed: *Metall. Trans. A*, 1988, vol. 19A, pp. 2741-52.
73. K.T. Park and F.A. Mohamed: *Metall. Trans. A*, 1990, vol. 21A, pp. 2605-08.
74. K.T. Park, S.T. Yang, J.C. Earthman, and F.A. Mohamed: *Mater. Sci. Eng. A*, 1994, vol. A188, pp. 59-67.
75. X.-G. Jiang, S.T. Yang, J.C. Earthman, and F.A. Mohamed: *Metall. Mater. Trans. A*, 1996, vol. 27A, pp. 863-72.
76. K.T. Park, J.C. Earthman, and F.A. Mohamed: *Phil. Mag. Lett.*, 1994, vol. 70, pp. 7-13.
77. S.T. Yang and F.A. Mohamed: *Metall. Mater. Trans. A*, 1995, vol. 26A, pp. 493-96.

78. A. Yousefiani and F.A. Mohamed: *Metall. Mater. Trans. A*, 1998, vol. 29A, pp. 1653-63.
79. A. Yousefiani, J.C. Earthman, and F.A. Mohamed: *Acta Mater.*, 1998, vol. 46, pp. 3557-70.
80. A. Yousefiani and F.A. Mohamed: *Phil. Mag. A*, 1999, vol. 79, pp. 1247-62.
81. A. Yousefiani and F.A. Mohamed: *Metall. Mater. Trans. A*, 2000, vol. 163A, pp. 163-72.
82. R.C. Gifkins: *Strength of Metals and Alloys*, R.C. Gifkins, ed., Pergamon, Oxford, United Kingdom, 1982, pp. 701-05.
83. T.H. Alden: *J. Aust. Inst. Met.*, 1969, vol. 14, pp. 207-16.
84. F.A. Mohamed: *J. Mater. Sci.*, 1983, vol. 18, pp. 582-92.
85. F.A. Mohamed: *J. Mater. Sci. Lett.*, 1988, vol. 7, pp. 215-17.
86. D. Mclean: *Metal Forum*, 1981, vol. 4, pp. 44-47.
87. M.P. Seah: *Acta Metall.*, 1977, vol. 25, pp. 345-57.
88. P. Gas, M. Guttmann, and J. Bernardini: *Acta Metall.*, 1982, vol. 30, pp. 1309-16.
89. E.A. Grey and G.T. Higgins: *Acta Metall.*, 1973, vol. 21, pp. 309-21.
90. P.A. Beck, J.C. Kremer, L.J. Demer, and M.L. Holzworth: *AIME Trans.*, 1948, vol. 175, pp. 372-94.
91. H. Hu and B.B. Rath: *Metall. Trans. A*, 1970, vol. 1, pp. 3181-84.
92. S. Wienig and E.S. Machlin: *AIME Trans.*, 1957, vol. 209, pp. 843-54.
93. J.W. Cahn: *Acta Metall.*, 1962, vol. 10, pp. 789-98.
94. K. Lücke and H.P. Stüwe: *Acta Metall.*, 1971, vol. 19, pp. 1087-99.
95. M.J. Mayo and W.D. Nix: *Acta Metall.*, 1989, vol. 37, pp. 1121-34.
96. R.C. Gifkins: *Scripta Metall.*, 1991, vol. 25, pp. 1397-1400.
97. B. Burton: *Diffusional Creep in Polycrystalline Materials*, Trans Tech Publications, Bay Village, OH, 1977.
98. F.A. Mohamed and J. Wolfenstine: in *Hot Deformation of Aluminum Alloys*, T.G. Langdon, H.D. Merchant, J.G. Morris, and M.A. Zaidi, eds., TMS, Warrendale, PA, 1991, pp. 223-37.
99. O.A. Ruano, J. Wadsworth, and O.D. Sherby: *Acta Metall.*, 1988, vol. 36, pp. 1117-28.
100. F.A. Mohamed, K.L. Murty, and J.W. Morris, Jr.: in *Rate Processes in Plastic Deformation of Materials*, J.C.M. Li and A.K. Mukherjee, eds., ASM, Metals Park, OH, 1975, pp. 459-77.
101. F.A. Mohamed and T.J. Ginter: *Acta Metall.*, 1982, vol. 30, pp. 1881-1982.
102. A.J. Ardell and S.S. Lee: *Acta Metall.*, 1986, vol. 34, pp. 2411-23.
103. A.J. Ardell: *Acta Mater.*, 1997, vol. 45, pp. 2971-81.
104. C.R. Barrett, E.C. Muehlesien, and W.D. Nix: *Mater. Sci. Eng.*, 1972, vol. 10, pp. 33-42.
105. S.V. Raj: *Scripta Metall.*, 1985, vol. 19, pp. 1069-73.
106. F.R.N. Nabarro: *Acta Metall.*, 1989, vol. 37, pp. 2217-22.
107. J. Weertman: *Trans. Am. Soc. Met.*, 1968, vol. 61, pp. 681-94.
108. J. Friedel: *Dislocations*, Pergamon Press, Oxford, United Kingdom, 1964.
109. T.G. Langdon and P. Yavari: *Acta Metall.*, 1982, vol. 30, pp. 881-87.
110. M.Y. Wu and O.D. Sherby: *Acta Metall.*, 1984, vol. 32, pp. 1561-72.
111. J. Weertman and J. Blacic: *Geophys. Res. Lett.*, 1984, vol. 11, pp. 117-20.
112. J.N. Wang and T.G. Langdon: *Acta Metall.*, 1994, vol. 42, pp. 2487-92.
113. J.N. Wang: *Acta Metall.*, 1996, vol. 44, pp. 855-62.
114. J.N. Wang: *Phil. Mag.*, 1995, vol. 71A, pp. 115-26.
115. F.A. Mohamed, K.L. Murty, and J.W. Morris, Jr.: *Metall. Trans.*, 1973, vol. 4, pp. 935-40.
116. T.J. Ginter, P.K. Chaudhury, and F.A. Mohamed: *Acta Mater.*, 2001, vol. 49, pp. 263-72.
117. B. Burton: *Phil. Mag.*, 1972, vol. 25, pp. 645-59.
118. W. Blum and W. Mailer: *Phys. Status Solidi (a)*, 1999, vol. 171, pp. 467-74.
119. J. Ginter and F.A. Mohamed: *Mater. Sci. Eng.*, in press.
120. J. Weertman: *Trans. TMS-AIME*, 1976, vol. 239, pp. 1989-2004.
121. R.C. Gifkins: *J. Inst. Met.*, 1958–59, vol. 87, pp. 255-61.